Chapter 6
Fabrication of Polyaniline Supported Nanocomposites and Their Sensing Application for Detection of Environmental Pollutants

Mohammad Shahadat, Mohammad Oves, Abid Hussain Shalla, Shaikh Ziauddin Ahammad, S. Wazed Ali, and T. R. Sreekrishnan

Abstract Nanoscale composite materials have played a significant role in sensing of gases, owing to their high surface area, higher mechanical strength with efficient chemical activity as well as cost effective nature. The present chapter deals with synthesis and characterization of Polyaniline (PANI) based nanocomposites ion-exchanger and nanomaterials in addition to their sensing applications in various fields. These nanomaterials have been explored on the basis of advanced techniques of characterizations. Besides the sensing materials, on the basis of ion uptake capacity, these nanocomposite ion-exchange materials can also be used for the treatment of meal ions from industrial wastewaters. This chapter mainly focuses on the synthesis of PANI based nanocomposites and their applications as gas sensors and biosensors. The PANI nanomaterials demonstrated impressive results and outstanding sensing behaviour. It has been found that PANI based nanocomposite materials are not only used for the detection of toxic gases, but, these materials

M. Shahadat (✉)
Department of Biochemical Engineering and Biotechnology, Indian Institute of Technology Delhi, New Delhi, India

Department of Textile Technology, Indian Institute of Technology Delhi, New Delhi, India

M. Oves
Centre of Excellence in Environmental Studies, King Abdul Aziz University, Jeddah, Saudi Arabia

A. H. Shalla
Department of Chemistry, Islamic University of Science & Technology (IUST), Pulwama, Jammu and Kashmir, India

S. Z. Ahammad · T. R. Sreekrishnan
Department of Biochemical Engineering and Biotechnology, Indian Institute of Technology Delhi, New Delhi, India
e-mail: sree@dbeb.iitd.ac.in

S. Wazed Ali
Department of Textile Technology, Indian Institute of Technology Delhi, New Delhi, India

M. Oves et al. (eds.), *Modern Age Waste Water Problems*,
https://doi.org/10.1007/978-3-030-08283-3_6

also facilitated immobilization of bioreceptors (e.g., enzymes, antigen–antibodies, and nucleic acids, etc.) for the exposure of biological agents through a combination of biochemical and electrochemical reactions. In future, PANI based nanocomposite materials are expected to open new approaches for demonstrating their outstanding applications in diverse fields.

Keywords Synthesis · Characterization · Polyaniline · Sensing behavior · Biosensors · Metal ions

6.1 Introduction

Recently, polyaniline (PANI) based organic–inorganic conducting nanocomposite materials have played important role in the field of nanotechnology. These nanocomposites with combinations of two or more components have received more and more attention, owing to their interesting physical properties as well as many potential applications in various areas (Gangopadhyay and De 2000). Conducting polymers are a new class of materials with essential applications in a different growing advance technologies, such as energy storage devices and chemical sensors (Novák et al. 1997; Santhanam and Gupta 1993; Feng and MacDiarmid 1999; Ayad et al. 2009; Singh et al. 2008; Sutar et al. 2007; Khan et al. 2010a; Jain et al. 2003; Fuke et al. 2008, 2009). In the development of nanocomposite materials, organic polymers such as polyaniline, polythiophene, polyacrylonitrile, etc. have been extensively used. Because of their significant proton dopability, these materials have the prominent features of variable electrical properties, low cost, ease of synthesis, excellent redox recyclability and thermal as well as chemical stability (Nabi et al. 2011a; Shahadat et al. 2015).

Among all conducting polymers, PANI has attracted much attention (Genies et al. 1990; Syed and Dinesan 1991; Huang et al. 1986; Shahadat et al. 2012) on account of its ability, under certain conditions to exhibit a high level of electrical conductivity (Adams et al. 1996; Shahadat et al. 2017). PANI demonstrates electrical conductivity because of their conjugated pi-bond system. These conjugated double bonds permit transfer of electron mobility throughout the molecule due to the delocalization of electron. Besides this, it is also considered as an environmentally stable and highly tunable conducting polymer which can be obtained in the form of bulk powder, cast films, or fibers. In conjunction with feasibility of low-cost, large-scale production, makes PANI an ideal candidate for various applications in different fields and therefore, can be successfully employed as a sorbent (Vatutsina et al. 2007) ion-exchanger (Nabi et al. 2010, 2011b, c; Bushra et al. 2014), catalyst (Arrad and Sasson 1989), ion selective electrode (Khan 2006) and sensor (Raman et al. 1996), conducting material (Shahadat et al. 2012) and also used in the host guest chemistry (Khan et al. 2011).

It is also observed that polymer is believed to be deprotonated by ammonia, which results change in conductivity of nanocomposite material (Khan et al. 2011). On the basis of alteration of conductivity, PANI based nanocomposite materials can be used towards sensing behaviour of ammonia. Determination of ammonia is essential for industrial, agricultural and medical fields together with environmental monitoring areas because ammonia is one of the critical industrial exhaust gas having high toxicity. In the scientific literature, a number of articles have been published that deals with the application of nanocomposite materials as a gas sensor. A number of metal oxides conjugated with PANI based ion-exchange materials have been demonstrated their sensing behaviour towards gases (Docquier and Candel 2002; Hu et al. 2002; Riegel et al. 2002; Ampuero and Bosset 2003; Dubbe 2003). The present book chapter reposts synthesis and characterization of PANI based nanocomposite ion-exchange materials and their sensing behaviour for the detection of gases.

6.2 PANI Based Nanocomposite Ion-Exchange Materials and Their Sensing Applications

The nanocomposite of polyaniline–titanium(IV)phosphate (PANI–TiP) was synthesized using a very simple sol–gel chemical route (Khan et al. 2011). The nanocomposite material was characterized on the basis of Fourier transform infrared spectroscopy (FTIR), thermogravimetric analysis (TGA), and scanning electron microscopy (SEM) analysis, the latter two confirmed smooth spherical morphology covered a particle size of ~25–45 nm. The material was examined to detect sensing at room temperature (25 ± 2 °C). Sensing behaviour measurement confirmed that nanocomposite of PANI–TiP demonstrated good reversible sensitivity towards ammonia (3–6%). Besides the doping of p-toluene sulphonic acid (p-TSA), a nanocomposite of PANI–TiP was also doped with hydrochloric acid (HCl) which demonstrated higher sensing response of p-TSA than HCl together with detection limit ≤1% ammonia. The higher electrical resistivity of the PANI-TiP nanocomposite may be attributed to the dopant p-toluene sulphonates consumed by NH_4^+ ions which make a weak charge complex of p-toluene ammonium sulphate ($C_7H_7SO_3 - NH_4^+$). In addition, it increases the resistivity of the nanocomposite, owing to the resistance in the mobility of the charge carriers along the backbone of the polymer. The weak charge complex starts to dissociate immediately as the sensor kept in the air and it regains its resistivity after a certain specific period. Hydrochloric acid also has the potential to form complex, however, ammonia molecule actively interacts with chloride ions which was not easily dissociated by putting the sensor in air (Koul and Chandra 2005). Proposed mechanism for complex formation of ammonia ($C_7H_7SO_3 - NH_4^+$) with PANI-TiP nanocomposite is shown in Scheme 6.1.

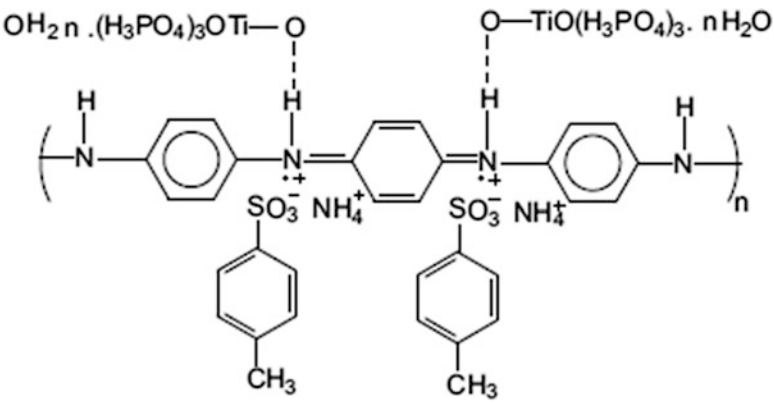

Scheme 6.1 Sensing behaviour of PANI-TiP nanocomposite ($C_7H_7SO_3 - NH_4^+$) towards ammonia. (Reprinted with permission, Khan et al. 2011)

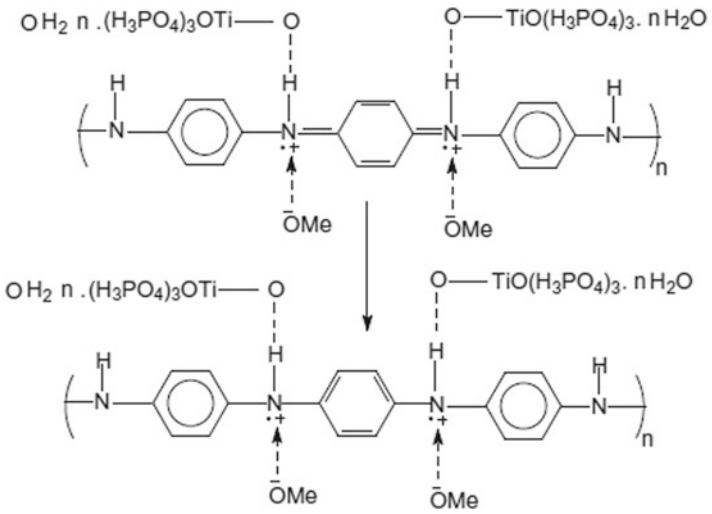

Fig. 6.1 Interaction of methanol with imine nitrogen of PANI. (Reprinted with permission, Khan et al. 2010b)

Same nanocomposite material (PANI–TiP) was synthesized to investigate the IEC, DC electrical conductivity and sensing behaviour towards alcohol vapors (Khan et al. 2010b). It exhibited good ion-exchange capacity and isothermal stability in terms of DC electrical conductivity retention at ambient conditions below 100 °C. Sensing characteristics of PANI–TiP nanocomposite towards alcohol was found to be higher than that of native PANI. The interaction between nanocomposite (PANI–TiP) and methanol molecule is shown in Fig. 6.1.

Nanofiber of V_2O_5@polyaniline was fabricated by in-situ oxidative polymerization of aniline in the presence of V_2O_5 and surfactant (cetyltrimethylammonium

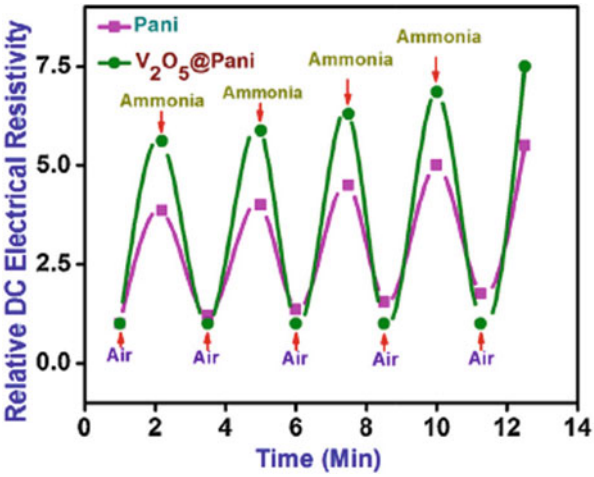

Fig. 6.2 Variation in the resistivity of pTSA-doped PANI and V2O5 composite nanofibers upon intermittent exposure of ammonia (0.1 M). (Reprinted with permission, Hasan et al. 2015)

bromide) (Hasan et al. 2015). Besides SEM, TEM, TGA-DTA and XRD analyses, the nanocomposite materials were also characterized by Raman spectroscopy, X-ray photoelectron spectroscopy. The DC electrical conductivity of V_2O_5@Pani composite nanofibers measured at 25 ± °C as 1.33 S cm^{-1}, which was found significantly higher than that the nanocomposite of HCl-doped PANI (Ansari et al. 2013). Under ambient conditions, the materials (pTSA-doped Pani and V_2O_5@Pani composite nanofiber) were examined to determine sensing response of ammonia vapour at low concentration (0.01 M). It was found that V_2O_5@pani nanofiber sensor demonstrates higher sensing response as compare to pTSA-doped PANI nanofiber sensor (which was fabricated in the presence of the surfactant; CTAB). Since, V_2O_5 (Ansari and Mohammad 2011) and PANI (Raj et al. 2010) independently exhibited ammonia sensing behaviour, however, V_2O_5@Pani nanocomposite showed higher sensing response owing to the synergistic/additional effect of both V_2O_5 and PANI as well as polymerization of aniline on V_2O_5 may increase the surface area of PANI, which result improvement in sensing response. A comparative study related to the sensing behaviour of both nanocomposites is shown in Fig. 6.2.

Chemical oxidative polymerization of 3-methythiophene (3MTh) in the presence of titanium(IV)molybdophosphate (TMP) has been carried out to synthesized poly (3-methythiophene)-titanium(IV)molybdophosphate (P3MTh–TMP) cation exchange nanocomposites (Khan and Baig 2013a). The characterization results confirmed a strong interaction between P3MTh and TMP particles which result higher thermal stability of P3MTh–TMP nanocomposites than pure P3MTh. The nanocomposite material showed good ion-exchange capacity, electrical conductivity, and isothermal stability under ambient condition below 100 °C. The results of sensing behaviour indicated enhancement in resistivity of nanocomposites on exposure to ammonia at room temperature (25 °C) and a linear relationship between the responses and the concentration of ammonia was achieved.

Electropolymerisation method was used for the fabrication of graphenated polyaniline/tungsten oxide (PANI/WO_3/GR/GCE) nanocomposite sensor on a graphene-modified glassy carbon electrode (Tovide et al. 2014). The electrode of PANI/WO_3/GR/GCE nanocomposite was examined for sensing behaviour of phenanthrene using cyclic voltammetry. It was found that PANI/WO_3/GR/GCE nanocomposite exhibited higher sensitivity towards phenanthrene and covered a dynamic linear range (1.0–6.0 pM) with a detection limit of 0.123 pM. In addition, it showed excellent reproducibility and long-term stability as well as lower detection in sensitivity than the WHO permissible limit (1.12 nM phenanthrene in wastewater. Advanced techniques namely Cyclic voltammetric (CVs), square wave voltammetric (SWVs), X-ray diffraction (XRD). Atomic force microscope (AFM) Raman spectra, Electrochemical impedance spectra (EIS) measurement and HRTEM and FTIR analyses were employed for the characterization of the nanocomposite. On the basis of good sensing response towards the detection of phenanthrene, PANI/WO_3/GR/GCE nanocomposite can be applied in a reactor for the degradation of PAHs with minimal energy requirement.

Chemically oxidative polymerization method was employed to prepare Polypyrrole-zirconium(IV)selenoiodate (PPy/ZSI) cation exchange nanocomposite (Khan et al. 2013a). The XRD pattern of the PPy, ZSI confirmed amorphous nature and SEM analysis indicated its globular surface. On the basis of EDX analysis the tentative structure of inorganic precipitate (ZSI) was found to be as $[(ZrO)_4(OH)(HSeO)_3(IO_3)_2]_n$. The ion-exchange capacity (IEC) and electrical conductivity of the nanocomposite was found to be 2.49 meq g^{-1} and 0.436 Scm^{-1} respectively. In terms of thermal stability, the nanocomposite demonstrated significant isothermal DC electrical conductivity retention up to 130 °C under ambient condition. The material was tested to determine the sensing behaviour of formaldehyde vapors at room temperature (25 ± 2 °C). It was found that the resistivity of PPy/ZSI increases with increasing percent concentration of formaldehyde at room temperature. Thus, PPy/ZSI based sensor showed good reversible response towards formaldehyde vapors in the range of 5–7%. In addition, the percentage composition of formaldehyde varpour was also measured in terms of mole fractions which was found to be 0.099%, 0.142% and 0.211% for 5, 7 and 10%, respectively. A schematic presentation related to the reversible interaction between PPy/ZSI and formaldehyde is shown in Fig. 6.3. This study confirms that PPy/ZSI based nanocomposite can be used as a smart sensor for the detection of formaldehyde.

Another electrically conducting Poly-o-toluidineetitanium(IV)phosphate (POT-TiP) cation exchange nanocomposite was fabricated by the mixing of Poly-o-toluidine and inorganic precipitate (titanium(IV)phosphate) (Khan and Baig 2013b). TEM analysis of POT-TiP nanocomposite confirmed its spherical morphology having an average particle size of 25–30 nm. The nanoparticles of TiP were shown in the form of dark spots dispersed in the matrix of poly-o-toluidine. The XRD pattern of POT-TiP showed its amorphous nature due to the dispersion of inorganic precipitate in the matrix of Poly-o-toluidine. In terms of conductivity, nanocomposite cation exchange material was examined to check humidity responses in the air. With increasing percentage of relative humidity, the resistivity of the

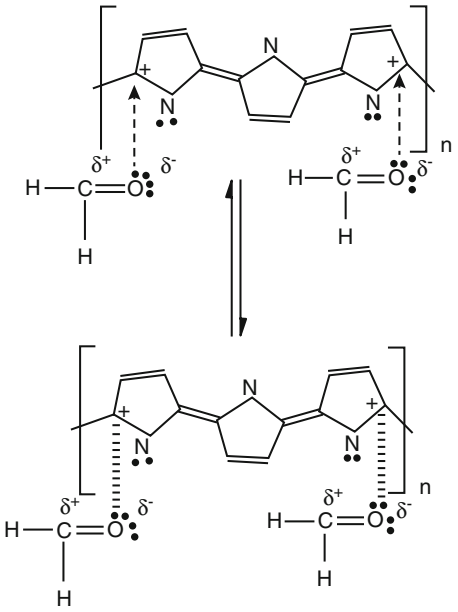

Fig. 6.3 A mechanistic representations for reversible interaction between PPy/ZSI and formaldehyde. (Reprinted with permission)

nanocomposite was found to be decreased. Improvement in conductivity or decline in resistivity with the enhancement of humidity can be attributed to the mobility of the dopant ion in the polymer matrix (Singla et al. 2007) which were loosely attracted to the chain of poly-o-toluidine by very weak forces (Van der walls forces of attraction). It was also found that at low humidity, the mobility of dopant was restricted due to dryness which curled polymer chain. In other words, at high humidity content, polymer chains become aligned with respect to each other. Decline in resistivity with increasing humidity content confirmed the adsorption of the water molecules, therefore, PANI chain of the nanocomposite act as a p-type semiconductor (the lone pair e increased, i.e., the concentration of hole^{-} from the conducting complex toward the TiP water molecules). The partial charge transfer process of conducting species with that of water molecules decreased the resistivity of nanocomposite as shown in Fig. 6.4. The nanocomposite material demonstrated good humidity response along with ion-exchange capacity and electrical conductivity. In terms of DC electrical conductivity retention, POT-TiP based nanocomposite was found stable under ambient conditions below 90 °C. Significant results of sensing behaviour towards humidity established that the POT-TiP can be employed as a good sensing material for detection of humidity.

To develop a new humidity sensor, poly-o-anisisine based poly-o-anisidine-Sn (IV) arsenophosphate (POA-SAP) nanocomposite has been synthesized by the sol-gel method (Khan et al. 2013b). Besides sensing behaviour, the ion-exchange property of the material was also determined to use it as a cation exchange material. Physico-chemical properties were also measured in terms of diffusion coefficient (D°), the energy of activation (E_a) and standard entropy change ($\Delta S°$). The humidity

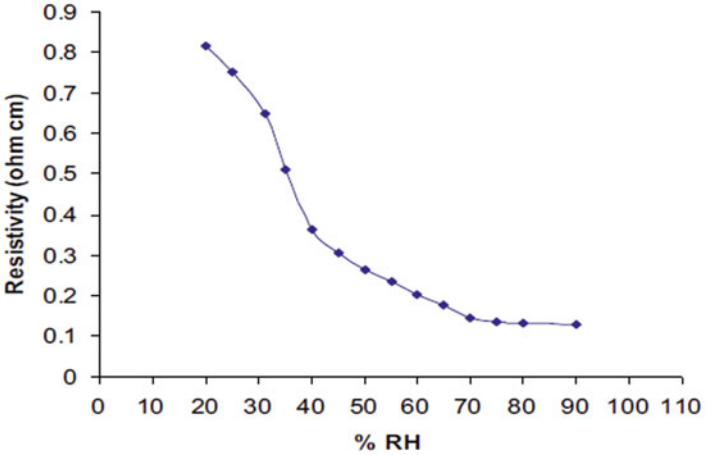

Fig. 6.4 Humidity response of Poly-o-toluidine-TiP cation exchange nanocomposite for 20–90% RH. (Reprinted with permission, Khan and Baig 2013b)

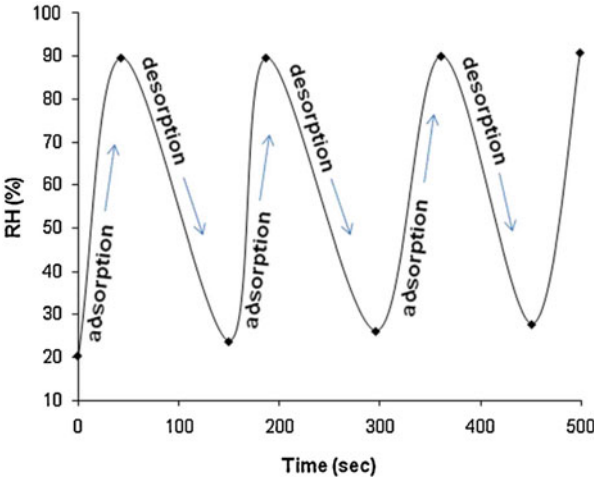

Fig. 6.5 Recovery response of humidity sensor (poly-o-anisidine Sn(VI) arsenophosphate nanocomposite cation exchanger). (Reprinted with permission, Khan et al. 2013b)

sensing (adsorption) and recovery (desorption) response of the nanocomposite was measured in the form of electrical conductivity with respect to time at 25 ± 2 °C (as shown in Fig. 6.5). The time response for continuous humidification was found 60 s (from 20 to 90% RH) and recovery time was achieved in 140 s. The long recovery time pointed out towards slow surface desorption process of water molecules at ambient temperature. Therefore, POA-SAP nanocomposite material showed an advantage for humidity sensing applications owing to its quick response and recovering characteristics.

Khan et al., fabricated PANI based electrically conductive polyaniline-titanium (IV)molybdophosphate (PANI-TMP) cation exchange nanocomposite for detection

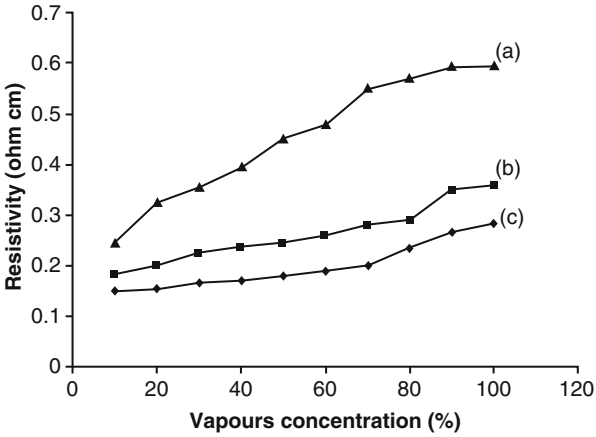

Fig. 6.6 Resistivity response of PANI-TMP nanocomposite towards (**a**) methanol (**b**) ethanol and (**c**) 1-propanol at different concentrations. (Reprinted with permission, Khan et al. 2013a)

of sensitivity towards the series of aliphatic alcohols (methanol, ethanol, and 1-propanol) (Khan et al. 2013a). The nanocomposite was prepared by the mixing of PANI with an inorganic precipitate of titanium (IV)molybdophosphate (TMP). Characterization was of the nanocomposite was performed on the basis of and FTIR, SEM, TEM, XRD, TGA, and UV-Vis. Comparative FTIR spectra of methanol exposed to PANI-TMP confirmed shifting of the quinoid peak from 1579 to 1547 cm^{-1} which attributed to the interaction of methanol with imine nitrogen, thereby causing the reducing effect. Therefore, the effective positive charge on imine nitrogen was reduced by the molecules of methanol. SEM analysis of PANI-TMP nanocomposite demonstrated its granular structure, and TEM image of PANI-TMP nanocomposite revealed spherical morphology which covered particle size in the range of 20–30 nm. The XRD pattern of PANI and TMP showed crystalline nature, however, after binding TMP with PANI, the morphology of nanocomposite became amorphous. TGA analysis of PANI-TMP nanocomposite confirmed its thermally stability than pure PANI and this nanocomposite can be used cover a wide range of temperature. In terms of resistivity, nanocomposite material was tested to examine its applicability as a sensor for aliphatic alcohols (methanol, ethanol, and 1-propanol). The resistivity response of the nanocomposite towards various concentrations of different alcohols has been determined (as shown in Fig. 6.6).

The reversible resistivity response of PANI-TMP for methanol, ethanol, and 1-propanol was also observed at 25 ± 2 °C. It is commonly known that PANI act as a p-type semiconductor; therefore, the exposure of electron-donating gases to PANI result decline in conductivity (Dimitriev 2003). The PANI-TMP sensor showed good reversible response towards methanol vapours compared to ethanol and 1-propanol vapours. These reversible resistivity responses were found to be due to the adsorption and desorption of the alcohol vapours. The reversible response for different concentration of methanol was also examined. It was found that the resistivity response increases with increasing methanol concentration (as shown in Fig. 6.7). The response time for continuous exposure of alcohol vapour was 20 s and

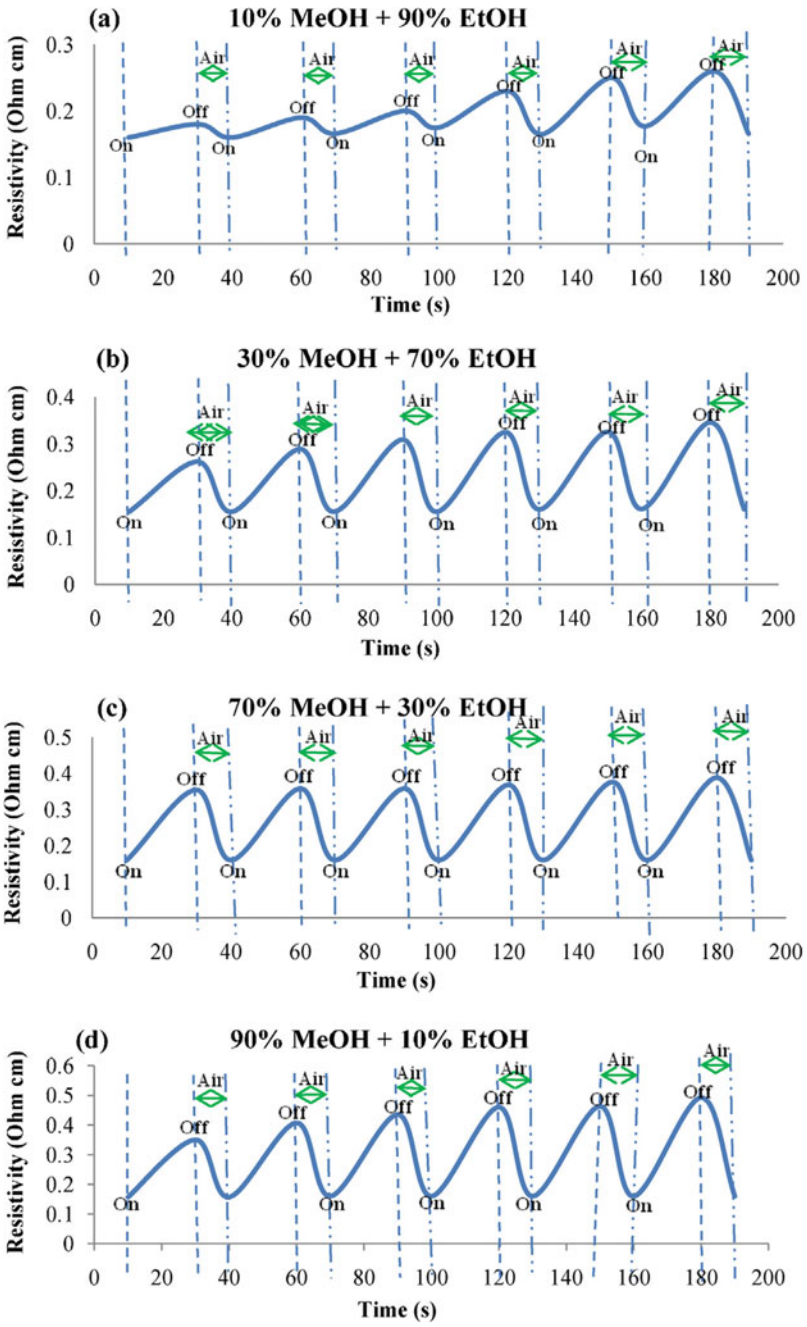

Fig. 6.7 Response transient curves of PANI-TMP nanocomposite towards different concentrations of methanol and ethanol mixture. (Reprinted with permission)

the recovery time out of the gas chamber was 10 s. The alteration in current–voltage data recorder confirmed that ethanol and 1-propanol vapours are less sensitive towards the PANI-TMP which may be due to the low polarity nature of ethanol and 1-propanol (Athawale and Kulkarni 2000). Owing to the small size and more polar nature of methanol molecules it can be efficiently interacted with nanocomposite material than other alcohols molecules (ethanol and 1-propanol). The response at each concentration justified that methanol molecules were found more sensitive and selective for PANI-TMP nanocomposite. PANI based nanocomposite demonstrated good resistivity response towards alcohol vapours; therefore, it can be used as a good sensing material for the detection of methanol vapours at room temperature.

Transition metal-supported (Cu^{2+}, Ni^{2+}, Co^{2+}, Fe^{2+}, and Mn^{2+}) polyaniline–zeolite (PANI-ZSM-5) nanocomposite ion-exchange material was synthesized and characterization was conducted by FTIR, XRD, TGA and SEM analyses (Kaur and Srivastava 2015). Sensing behaviour of PANI-Nano-ZSM-5 was examined for the detection of epinephrine, paracetamol, and folic acid. Among all synthesized materials, Cu^{2+}-PANI-ZSM-5 demonstrated the highest electro-catalytic activity together with excellent stability, sensitivity, and selectivity. Under equilibrium, epinephrine, paracetamol and folic acid covered a wide linear range (10 nM–600 M, 15 nM–800 M and 13 nM–700 M, respectively). The limit of detection for epinephrine, paracetamol, and folic acid was found as 4, 8, and 5 nM, respectively. On the basis of significant performance, the Cu^{2+}-PANI-ZSM-5 sensor can be applied for the determination of epinephrine, paracetamol, and folic acid in the commercial pharmaceutical preparations.

Another HCl doped multi-walled carbon nanotube (MWCNT)/polyaniline (PANI) nanocomposites based Pani@MWCNT nanocomposite ion-exchange sensor was prepared in the presence of surfactant (cetyl-trimethylammonium bromide) using in-situ oxidative polymerization of aniline (Ansari et al. 2014). The stability of the sensor was determined based on electrical conductivity retention under isothermal and cyclic aging conditions (as shown in Fig. 6.8).

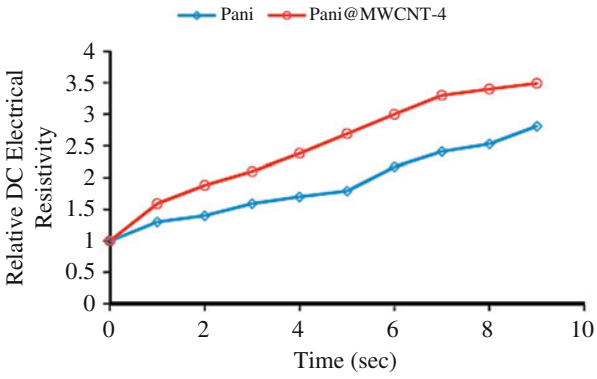

Fig. 6.8 Effect on the resistivity of HCl doped Pani and Pani@MWCNT-4 nanocomposite on exposure to ammonia (0.1 N) with respect time of exposure. (Reprinted with permission, Ansari et al. 2014)

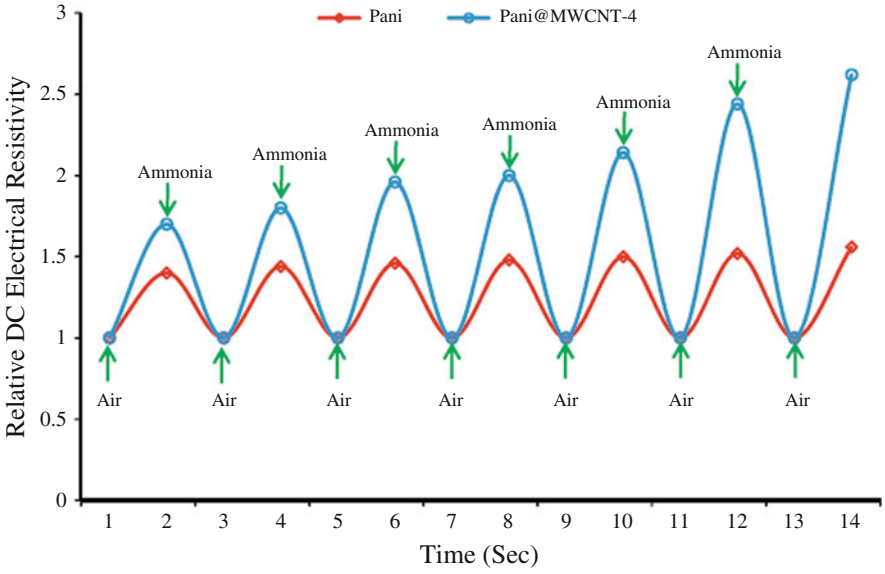

Fig. 6.9 Variation in resistivity of HCl doped (**a**) Pani and (**b**) Pani@MWCNT-4 nanocomposite on intermittent exposure to ammonia (0.1 N). (Reprinted with permission, Ansari et al. 2014)

On the basis of good isothermal and cyclic stability, nanocomposite sensor was tested for detection of ammonia sensing behaviour (Ansari et al. 2014). Relative resistivity of nanocomposite increased linearly on the exposure of ammonia and the resistivity did not reach to its initial value on exposure under ambient condition (Fig. 6.9). Excellent sensing response of Pani@MWCNT-4 can be attributed to the high surface area of PANI coated over MWCNTs. A proposed mechanism related to sensing behaviour of nanocomposite for the detection of ammonia vapor is shown in Fig. 6.10. Abudllah et al., also synthesized PANI/MWCNTs based nanocomposite for trace level detection of ammonia (NH_3) gas (Abdulla et al. 2015). The gas sensor behaviour of C-MWCNT and PANI/MWCNTs nanocomposite for detection of NH_3 gas at trace level (2–10 ppm) under ambient conditions were determined, and their performances were compared. It was examined that in terms of response and recovery time, PANI/MWCNTs nanocomposite based sensor showed significant sensitivity towards NH_3 gas in few seconds (6 s), which confirmed potential application of PANI/MWCNTs for detection of NH_3 in trace level.

A novel layer-by-layer (LBL) deposition technology was used for the fabrication of layered double hydroxide (LDH)/conductive polymer multilayer films by the alternate assembly of exfoliated ZnAl-LDH nanosheets and polyaniline (PANI) on silicon wafer substrates (Xu et al. 2013a). UV–vis absorption spectroscopy measured the regular growth of the (LDH/PANI)n multilayer films upon increasing deposition cycles. Uniform surface and thickness (2 nm per bilayer) of the nanocomposite was determined by SEM and AFM analyses. Multilayer films of $(LDH/PANI)_n$ nanosheets demonstrated a highly selective response to ammonia at

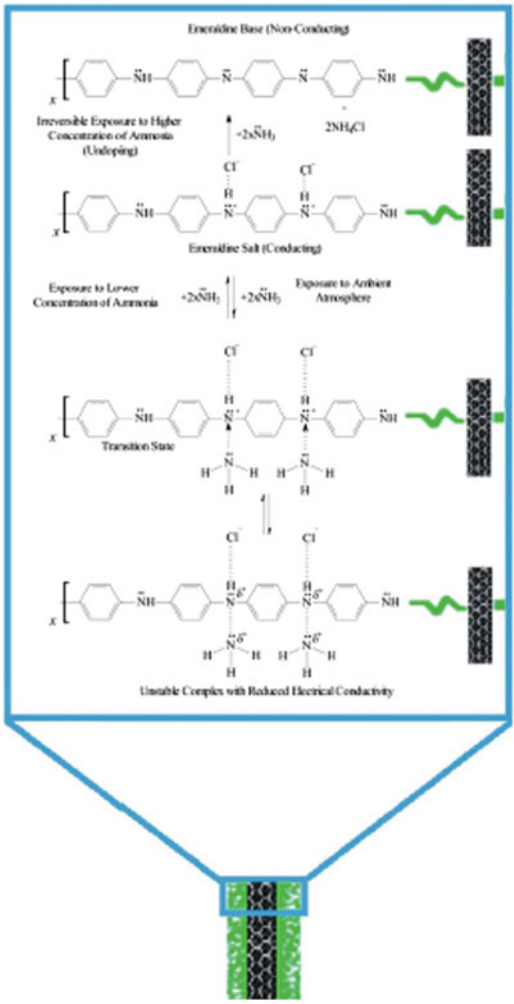

Fig. 6.10 Proposed mechanism for the ammonia vapor sensing for Pani@MWCNT nanocomposites. (Reprinted with permission)

room temperature (25 ± 2 °C) due to the existence of LDH in nanosheets. It can be seen that all the $(ZnAl\text{-}LDH/PANI)_n$ multilayer films have a reversible response to NH_3 at room temperature. The experiment was conducted by exposing the multilayer films for 90 s in the air, and the air was replaced by 1000 ppm ammonia and kept it for 450 s before the environment was switched back to air. The response values to ammonia (1000 ppm) increased from 14 to 16 by increasing bilayers numbers (from 12 to 30). The response and recovery time of $(ZnAl\text{-}LDH/PANI)_{12}$ at room temperature were found to be 120 and 150 s, respectively, however, for $(ZnAl\text{-}LDH/PANI)_{30}$, though the response increases from 14 of $(ZnAl\text{-}LDH/PANI)_{12}$ multilayer film to 16, the response/recovery are prolonged to 150/240 s (as shown in Fig. 6.11).

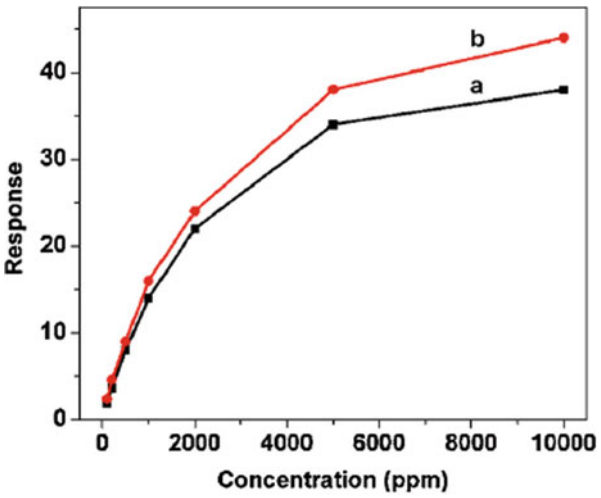

Fig. 6.11 Responses of (ZnAl-LDH/PANI)n multilayer film to different concentration of ammonia at room temperature ((**a**) n = 12 and (**b**) n = 30). (Reprinted with permission, Xu et al. 2013a)

The response of gas sensors can be changed by altering the concentration of ammonia at a constant temperature. In addition, multilayer films can also be detected ammonia gas below100 ppm, and the corresponding values were found to be as 1.8 and 2.4 for $(ZnAl\text{-}LDH/PANI)_{12}$ and $(ZnAl\text{-}LDH/PANI)_{30}$, respectively. The responses of multilayer films surprisingly improved with increasing concentration of NH_3 and the value of responses were found to be 3.6, 8, 14, 22, 34 and 38 for $(ZnAl\text{-}LDH/PANI)_{12}$ multilayer film to 200, 500, 1000, 2000, 5000 and 10,000 ppm ammonia, and the corresponding values for $(ZnAl\text{-}LDH/PANI)_{30}$ multilayer film are 4.6, 9, 16, 24, 38 and 44, respectively, Thus, LDH nanosheets play an essential role to improve the gas sensing properties of PANI because ZnAl-LDH nanosheets provide a rigid, confined and stable microenvironment. The uniform orientation and a suppressed aggregation of nanosheets may increase the void for reaction with ammonia molecule, and the ammonia sensing response primarily enhanced. To determine selective behaviour of $(ZnAl\text{-}LDH/PANI)_{12}$ and $(ZnAl\text{-}LDH/PANI)_{30}$ multilayer film with respect to different gases as (NO_2, CO, H_2, CH_4, C_2H_2 and C_2H_5OH) upto 10,000 ppm, (which is ten times concentration of ammonia), their responses were compared with the response of the sensor toward ammonia (Fig. 6.12). It was observed that both multilayer films demonstrated high response towards ammonia, however, low responses were found for NO_2, CO, H_2, and no significant response achieved for CH_4, C_2H_2, and C_2H_5OH even with increasing concentration (ten times) of ammonia which indicated that the multilayerfilms of $(ZnAl\text{-}LDH/PANI)_n$ could be employed as good candidates for detection of ammonia.

Another polyaniline–titanium dioxide based PANI/TiO_2 nanocomposite was synthesized in the presence of colloidal TiO_2 using in-situ chemical oxidation polymerization approach (Tai et al. 2007). Prepared PANI/TiO_2 nanocomposite was mounted on a silicon substrate covered with interdigital electrodes to fabricate a gas sensor via the self-assembly method. Surface morphology of nanocomposite

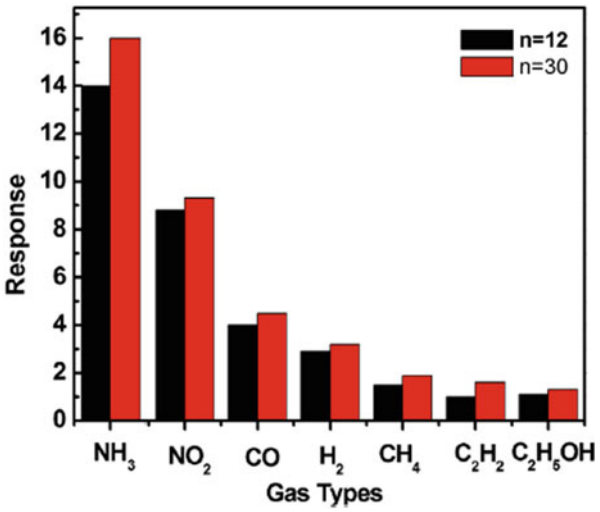

Fig. 6.12 Gas responses of $(ZnAl\text{-}LDH/PANI)_n$ multilayerfilms to 1000 ppm of ammonia and 10,000 ppm of NO_2, H_2, CO, CH_4, C_2H_2 and ethanol at room temperature. (Reprinted with permission, Xu et al. 2013a)

was examined by SEM analysis as shown in Fig. 6.13. It is evident from SEM image that a number of pores on the surface of nanocomposite were found which seem to contribute short response time and good reversibility of the sensors. Therefore, diffusion of gas occurs more readily in porous structures, and the reaction between gas molecules and the thin film occurs rapidly (Matsuguchi et al. 2002). However, the size of pores on the PANI/TiO_2 thin film (a) was much larger than the pure PANI film (b), which significantly improved the diffusion owing to its larger exposure area and penetration depth for gas molecules. Therefore, the response values of the PANI/TiO_2 thin film sensor increased due to its high surface-to-volume ratio to a degree (Sadek et al. 2006).

The material was used to examine gas-responses of NH_3 and CO. It was found that in terms of response, reproducibility and stability, a nanocomposite of PANI/TiO_2 demonstrated sensing behaviour towards NH_3 that was superior to CO gas. It was also found that as compared with NH_3 and CO gases, humidity was found less active on the resistance of the PANI/TiO_2 thin film. On the basis of SEM analysis, the microstructure of the PANI/TiO_2 nanocomposite demonstrated good agreement with the sensor performance. It was revealed that the difference gas sensing properties of pure PANI and PANI/TiO_2 thin films was occurred due to the alternation in surface the morphology.

In-situ oxidation polymerization of m-aminophenol was carried out in the presence of Carboxyl-functionalized multi-walled carbon nanotube (c-MWCNT) to synthesis PmAP/c-MWCNT nanocomposite (Verma et al. 2015). Interaction between the conjugated PmAP chain and the π-bonded surface of c-MWCNT was established by FT-IR and Raman spectroscopy. The surface morphology of the PmAP/c-MWCNT nanocomposite film was characterized by SEM and TEM analyses which demonstrated globular (spherical) microstructure of the PmAP deposited on the surface of c-MWCNT. The globular PmAP particles are consisting of

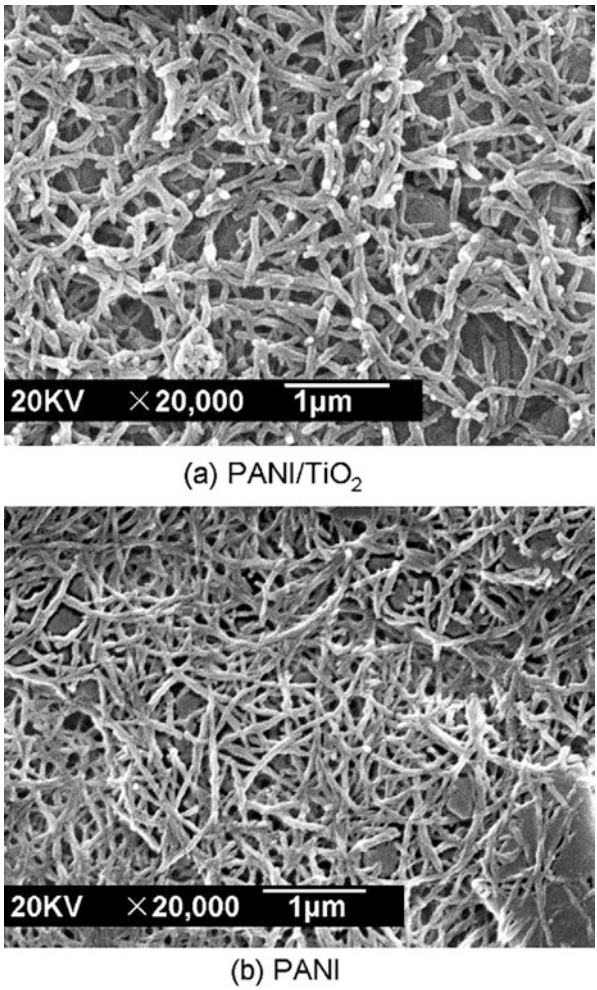

Fig. 6.13 SEM images of PANI/TiO_2 (**a**) and PANI (**b**) thin films. (Reprinted with permission, Tai et al. 2007)

considerable number of polymer chains. The XRD pattern of pure PmAP exhibits a broad amorphous diffraction peak which confirmed the amorphous nature of PmAP owing to periodicity parallel to polymer chain (Fig. 6.14). In addition, the PmAP/c-MWCNT nanocomposites demonstrated several sharp diffraction peaks that symbolized the crystalline nature of the PmAP. On increasing concentration of c-MWCNTs, the electrical resistance of the PmAP is significantly decreased to 11.6, 1.9, 0.25, and 0.06 kΩ cm for the PmAP/c-MWCNT nanocomposite containing 0.5, 1.0, 1.5 and 2.0 wt% c-MWCNT, respectively. The increase of conductivity can be attributed to the strong π–π* electron/H-bonding interactions between the c-MWCNTs and PmAP chains, leading to the formation of highly ordered crystalline nature of PmAP matrix that in turn decreased the resistance of the nanocomposite.

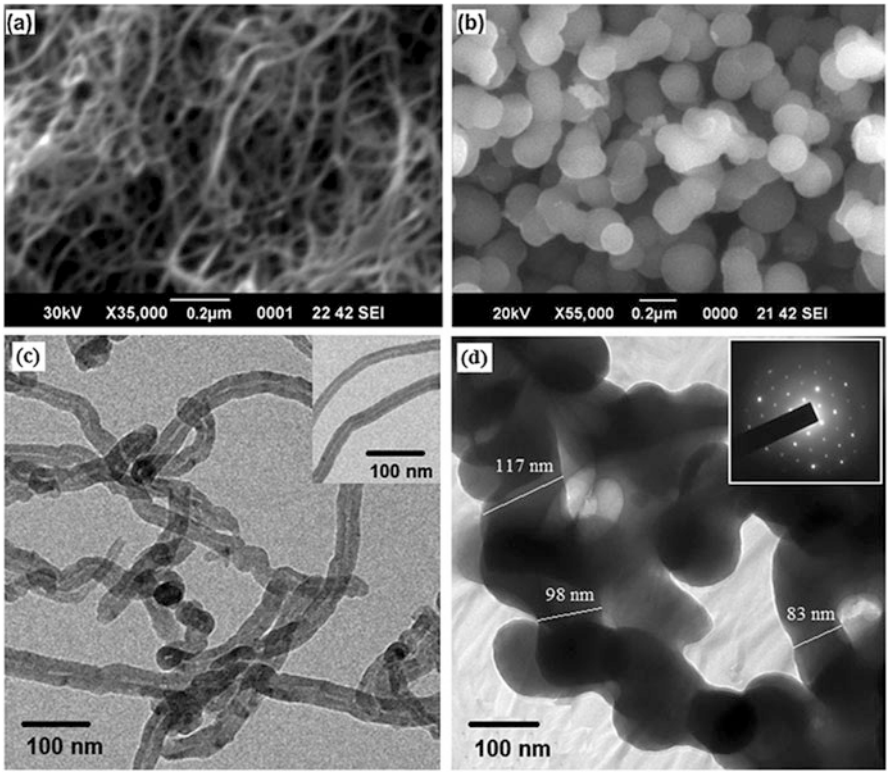

Fig. 6.14 SEM (**a** and **b**) and TEM images of carboxyl-functionalized MWCNTs and 2 wt% c-MWCNT contained PmAP/c-MWCNT nanocomposite. Inset of the figure (**d**) represents electron diffraction pattern of the nanocomposite. (Reprinted with permission, Verma et al. 2015)

The incorporation of c-MWCNTs with the matrix of PmAP matrix substantially improve the alcohol sensing potential of PmAP at relatively lower vapor concentration consequently the synergic effects of the components. Increasing concentration of c-MWCNTs enhanced the dynamic responses of different PmAP/c-MWCNT nanocomposites toward methanol and ethanol vapor at 90 ppm. The absorption of alcohol molecules successfully altered the electrical conduction of the PmAP/c-MWCNT. The extent of alcohol absorption and subsequent change in electrical resistance were dependent on the incorporation of c-MWCNT in the matrix of PmAP/c-MWCNT.

Oxidative polymerization of aniline was carried out in the presence of finely divided In_2O_3 to synthesize a PANI/In_2O_3 nanocomposite (Sadek et al. 2006). Prepared nanocomposite material was used to develop a surface acoustic wave (SAW) sensor was developed for the examination of sensing behaviour of different gases. The dynamic response to a sequence of various gases (H_2, CO, and NO_2) by varying concentrations in the synthetic air was determined (as shown in Figs. 6.15, 6.16 and 6.17). In synthetic air, the measured sensor responses were found

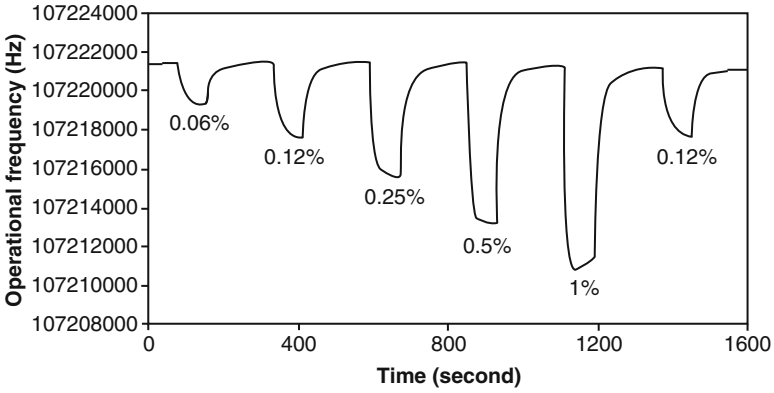

Fig. 6.15 Dynamic response of the SAW sensor towards different concentrations of H_2 at room temperature. (Reprinted with permission, Sadek et al. 2006)

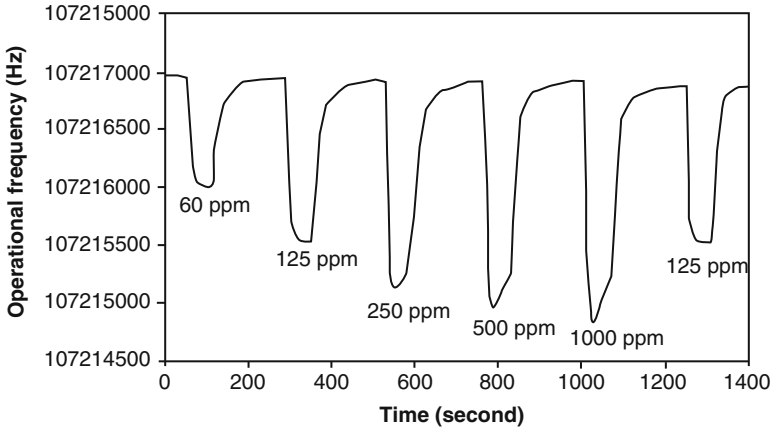

Fig. 6.16 Dynamic response of the SAW sensor towards different levels of CO at room temperature. (Reprinted with permission, Sadek et al. 2006)

approximately 11.0, 2.0 and 2.5 kHz towards 1% H_2, 500 ppm CO and 2.12 ppm NO_2, respectively. In addition, 90% response times; 30, 24 and 30 s was achieved for H_2, CO, and NO_2, respectively and the corresponding 90% recovery times were 40, 36 and 65 s. It was also found that, as compared to high concentration, the slower response was achieved at low density for all gases (H_2, CO, and NO_2). Thus, a high gas exposure time is required to get a stable sensing response (frequency shift) at low concentration. Reproducibility test was also performed to examine repeatability of nanocomposite by applying a second pulse of 0.12% H_2, 125 ppm CO and 510 ppb NO_2 into the sensor chamber which indicated that except for NO_2, PANI/In_2O_3 nanofibre based sensor has the potential to generate repeatable responses of the same magnitude with good baseline stability for H_2 and CO gases.

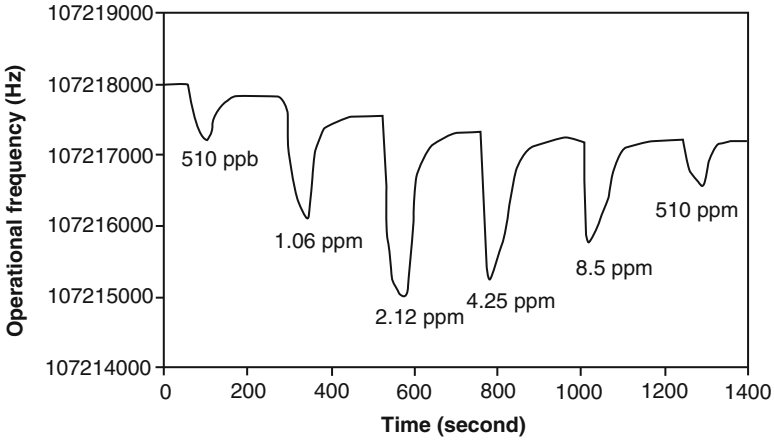

Fig. 6.17 Dynamic response of the SAW sensor towards different concentrations of NO_2 at room temperature. (Reprinted with permission, Sadek et al. 2006)

Reproducibility was observed as indicated when the second pulse of 0.12% H_2, 125 ppm CO and 510 ppb NO_2 was introduced into the sensor chamber. The PANI/In_2O_3 nanofibre based sensor produces repeatable responses of the same magnitude with good baseline stability for H_2 and CO gases, however, not for NO_2. Repeatability of the nanocomposite was confirmed by testing the sensor continuously over a period of 5 days. It was found that from the dynamic response curve of gases (frequency shift) increases almost linearly by increasing concentration of H_2, however, the frequency shifts for CO and NO_2 gases covered a nonlinear trend. For NO_2 gas, sensor response was not repeatable, and baseline seems to drift downward (at 4.25 and 8.5 ppm NO_2 concentration). The sensor response magnitude was found lower at 2.12 ppm which confirmed that high level of NO_2 gas is poisoning for the nanocomposite film. Thus, on the basis of fast response and recovery times with excellent repeatability, PANI/In_2O_3 nanocomposite could be used as a good sensing material for detecting H_2, CO and NO_2 gases at room temperature.

Ultrathin films of conducting polymers; Polyhexylthiophene (PHTh), poly(ethylene dioxythiophene) (PEDT), PHTh–PEDT copolymer, sulfonated polyaniline, polyaniline (PANI)–SnO_2, polypyrrole (PPy)–SnO_2, PEDT-SnO_2, PHTh–SnO_2 and copolymer (HTh-EDT)–SnO_2 were fabricated to examine sensing behaviour of gases (Ram et al. 2005a). The physical properties of films were investigated in terms of UV and FTIR analyses before and after the NO_2 gas treatment. The sensitivity of gases was measured in terms of resistance of PHTh, PEDT, PHTh–PEDT (as shown in Fig. 6.18). The value of resistance decreases exponentially upon exposure to NO_2 which established dopant nature of gas for conducting polymer. The films showed excellent reproducibility due to its thin nature. Among all synthesized nanocomposites and its copolymer P(HTh-PEDT), metal oxide nanocomposites films demonstrated the detection potential of NO_2 gas with high sensitivity.

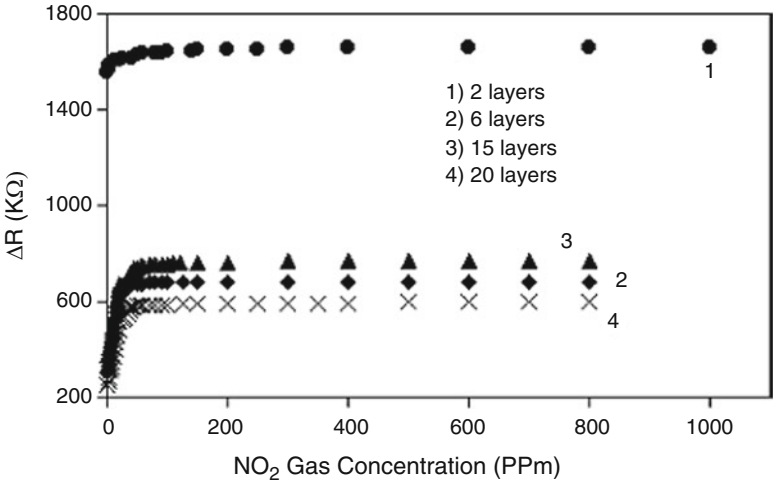

Fig. 6.18 Resistance change vs. NO_2 gas concentration along with a number of layers. (Reprinted with permission, Ram et al. 2005a)

Novel PANI based PANI/Mn_3O_4 composite material was fabricated to determine its sensing behaviour towards relative humidity. The material was doped with perchloric acid, sulphuric acid, *ortho*-phosphoric acid, acetic acid and acrylic acid to examine alteration in sensitivity with respect to relative humidity (Singla et al. 2007). On increasing relative humidity, the resistance of each polyaniline/Mn_3O_4 increased. The response of each composite was found to be almost linear with the percentage of relative humidity. However, the composites doped with organic acids showed more sensitivity than those with inorganic dopants. Under the identical conditions, these samples demonstrated reverse behaviour, and the value of resistance decreased with increasing relative humidity. This anomalous behaviour of the acid doped composite material may be due to lowering p-type nature of the polymer chains with the enhancement in humidity. Therefore, owing to the improvement in the resistance of composite materials doped with organic acids, it can act as a humidity sensor.

Titanium and polytetrafluoroethylene (Ti–PTFE) nanocomposite thin films were synthesized on glass substrates by the combination of dc and rf magnetron sputtering (Rujisamphan et al. 2016). Prepared Ti–PTFE composites below the percolation threshold (i.e., 27% metal volume filling (F)) produced Ti clusters with the average sizes of 7 ± 2 nm. The percolation threshold ($F = 62\%$) of nanocomosite increased with increasing the % of Ti content, the connecting regions of Ti were formed within the polymer matrix. The electrical conductivity of nanocomposite changed rapidly from insulator-like to metal-like properties. The Ti–PTFE composites prepared near the percolation threshold showed sensitivity in terms of electrical response towards different volatile organic compounds (VOCs). The sensitivities of Ti–PTFE device to acetone and ethanol as a function of VOCs concentration are shown in Fig. 6.19. It was observed that the sensitivity of acetone and ethanol increased with increasing

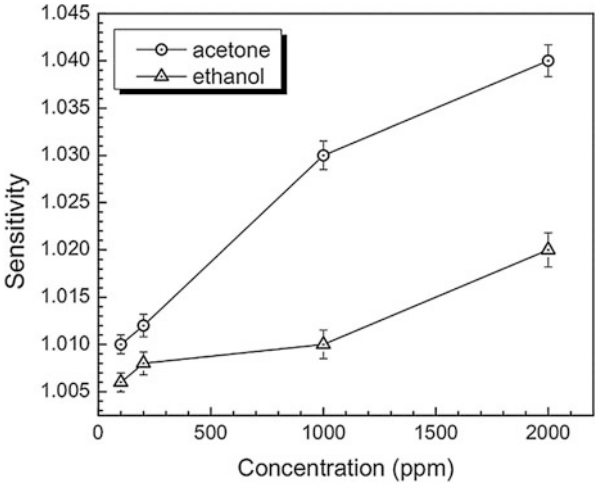

Fig. 6.19 Sensitivity of Ti–PTFE composite films for VOCs (acetone and ethanol). (Reprinted with permission, Rujisamphan et al. 2016)

VOCs concentration leading to higher changes in resistance. The sensing behaviour of nanocomposite towards acetone vapour was found to be higher than that of ethanol which may be due to different degrees of swelling on the polymer matrix. Thus, a number of factors including chemical bonding of the polymer, degree of crosslink, the concentration of metal nanoparticles including chemical reaction at the surface affect the degree of swelling. Other physico-chemical property namely; chemisorption on the TiF/TiO_2 clusters on the surface and a change in a composite structure might play significant role in the swelling mechanism. The sensitivities towards acetone vapor were found to be in the range of 1.01–1.04 corresponding to concentrations between 100 ppm and 2000 ppm. The XPS analysis confirmed the existence of chemical bonds (C C, C CF, C F and CF_2 and TiF) on the surface of TiO_2. Surface morphology was evaluated by AFM analysis demonstrated RMS surface roughness of nanocomposite as 13.3 nm. The particle size of Ti clusters dispersed in the PTFE matrix was found in the range of 10–30 nm (using TEM analysis).

Sensing behaviour towards the water, methanol, toluene, were investigated by synthesized carbon nanotube (CNT) grafted with poly(ε-caprolactone) (PCL) by layer by layer spray from PCL–CNT solutions (Castro et al. 2009). Grafting of ε-caprolactone on the CNT surface through in-situ ring opening polymerisation was performed usingNMR analysis after solvent extraction of ungrafted chains. The mechanism of grafting between the hydroxyl groups of the CNT surface and the aluminium-based catalyst leads to the formation of an intermediate compound. It has a potential to initiate a ring-opening polymerisation of ε-CL for the synthesis of the CPC in which PCL chains were grafted on CNT via covalent bonding (as shown in Fig. 6.20).

AFM analysis evaluated CNT coating and dispersion level. It was observed that commercial PCL led to less conductive CPC as compared to synthesized PCL which may be due to the low molar mass PLCs chains which can more effectively interact

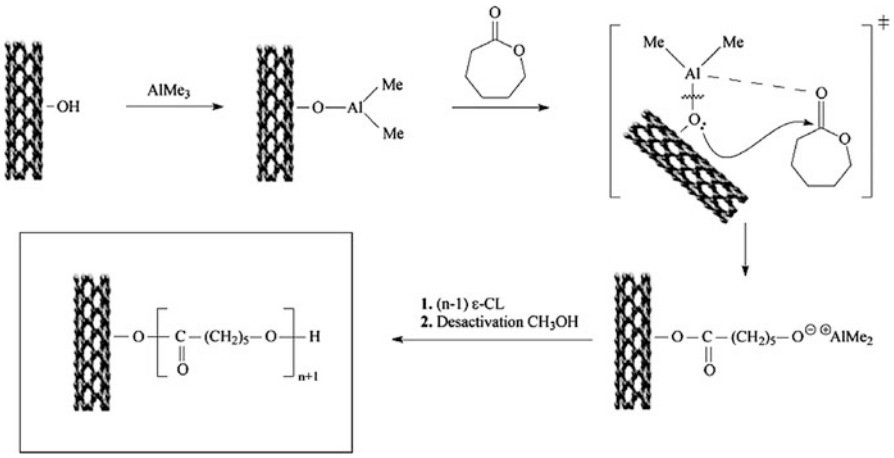

Fig. 6.20 Schematic representation of different steps leading to PCL-g-CNT CPC. (Reprinted with permission, Castro et al. 2009)

with PCL-g-CNT, leading to good dispersion and finally stabilizing the conducting network of nanocomposite. In terms of signal sensitivity, selectivity, reproducibility, and stability, the electro-chemical properties of Conductive Polymer Composite (CPC) sensors were analyzed towards sensing behaviour of water, methanol, toluene, tetrahydrofuran and chloroform vapours which resulted in the improvement in the sensor response using PCL grafted CNT (PCL-g-CNT). It was observed that for methanol vapour, CPC responses showed low amplitude below 1, whereas, it could reach up to 6 or even more than 100 for toluene and chloroform vapours, respectively. The ranking of the resistance relative amplitude (A_R) for all CPC followed the order: water < methanol < toluene < tetrahydrofuran << chloroform. Thus, CNT based PCL-g-CNT can be employed as a smart sensing material towards the sensitivity of water, methanol, and toluene.

Polyaniline-tungsten based nanocomposite materials with honeycomb like morphology was synthesized using in situ one pot chemical oxidative method (Chaudhary and Kaur 2015). A cost-effective spin coating technique was employed to fabricate sensing device for the monitoring of SO_2 at levels as low as 5 ppm at room temperature. FTIR and UV-Vis. established the formation of heterojunctions which led the enhancement in sensing response of hybrid nanocomposite. The sensing response of the nanocomposite based sensing device was found to be higher (~10.6%) as compared to its parent devices (~4% for polyaniline nanofibres and is negligible for tungsten oxide nanostructures) towards SO_2 (10 ppm). Enhancement in sensitivity may be due to the optimum porosity, branched structure and formation of heterojunctions of the nanocomposite. Gas sensing behaviour of PANI was found to be entirely different in comparison to the inorganic semiconductor. In PANI, the mechanism of SO_2 sensing may be explained regarding charge compensation

between the p-PANI and the electron acceptor (SO_2). The electrons were transferred from the p-PAN to the electron accepting SO_2 by the interaction of PAN with SO_2 which decline the resistance of PANI. Alternatively, metal oxides (WO_3), grains are always covered with adsorbed oxygen (O_2) molecules which captured electrons from the conduction band of the metal oxide, resulting formation of a chemisorbed oxygen species (O_2^-, O^- and O^{2-}) depending upon the sensor's operating temperature. Below 100 °C, the oxygen ions exist in O_2^-, however, other forms (O^- and O^{2-}) was also achieved above 100 °C. By exposing nanocomposite material to sulphur dioxide gas, the molecules of SO_2 extract electrons from the conduction band of WO_3, and react with O_2 which increases the width of the depletion layer and a decreased the conductivity of sensor. It was the first attempt to use PANI-WO_3 nanocomposite as a sensor for monitoring SO_2 at room temperature. Thus, PANI based cost effective nano-hybrid sensor has the potential to consume low power can be easy to fabricate and possesses all the essential characteristics of a reliable sensing device.

Polypyrrole base; PPy/a-Fe_2O_3 hybrid nanocomposite was synthesized by varying weight percentages (10–50%) of CSA (Navale et al. 2014). Nanomaterial was deposited on glass substrates using a spin coating technique to employ it as a sensing material. Morphological characterization of material was performed using XRD, FESEM, and TEM analyses (Fig. 6.21). Thin films of CSA doped PPy/aFe_2O_3 nanocomposite were examined towards the sensing behaviour of NO_2, Cl_2, NH_3, H_2S, CH_3OH and C_2H_5OH gases. Among all gases, nanocomposite material was found to be highly sensitive and selective for NO_2 gas at room temperature (i.e., with a chemiresistive response of 64% at 100 ppm with a reasonably fast response time of 148 s). FESEM micrograph of PPy/a-Fe_2O_3 hybrid nanocomposite (30% CSA doped) showed spherical granular morphology. The high porosity of PPy/a-Fe_2O_3 provides a high surface area to volume ratio and gas diffusion. Therefore, increasing the reaction between gas molecules and the surface of the films excepted to be a higher sensing responses (Tai et al. 2007; Wang et al. 2012). TEM image of PPy/a-Fe_2O_3 nanocomposite thin film demonstrated approximately spherical shaped nanoparticles in aggregated form. The dark shaded a-Fe_2O_3 nanoparticles were embedded into a light shaded matrix of PPy with an average diameter of 32 nm.

Gas sensing response of PPy/aFe_2O_3 hybrid nanocomposite thin films (30% CSA doped) for the detection of NO_2 gas with different concentrations (5–100 ppm) at 25 ± 2 °C indicated that the gas response increases linearly by increasing level of NO_2 gas (from 5 ppm to 100 ppm) and the reaction of CSA doped PPy/a-Fe_2O_3 sensor was found to 7%, 12%, 14%, 26%, 40%, 55% and 64%. Over 100 ppm NO_2 gas concentration, the response of the sensor was remained constant, which confirmed the equilibrium state of the nanocomposite sensor (Hsu et al. 2008). On the basis of the above finding, 100 ppm is considered as an optimum or saturated concentration for the adsorption of a NO_2 gas. The higher response of NO_2 gas can be explained on the basis of different surface interactions between active layer of the film and adsorbed gas (NO_2). The lower concentration of NO_2 result in the lower

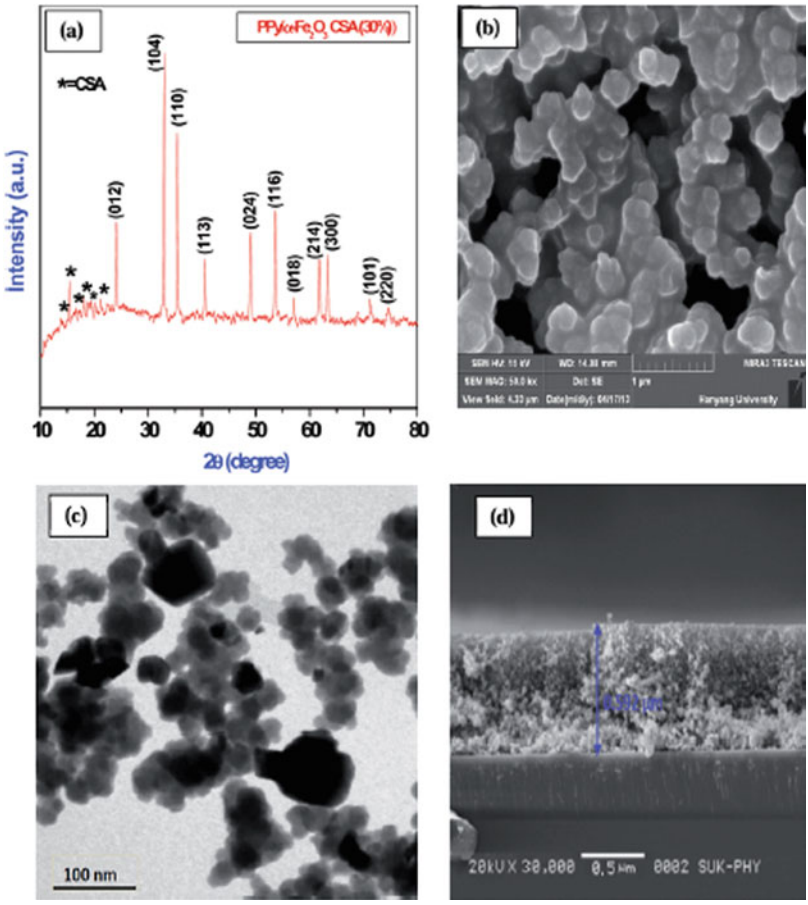

Fig. 6.21 (**a**) XRD pattern of CPF (30%) hybrid nanocomposite, (**b**) FESEM image of CPF (30%) nanocomposite thin film, (**c**) TEM image of CPF (30%) nanocomposite thin film and (**d**) cross-section SEM image of CPF (30%) nanocomposite thin film. (Reprinted with permission, Navale et al. 2014)

surface covered by gas molecules which reduced surface interactions between NO_2 gas molecules and coating of nanocomposite film. Thus, the maximum gas response (64%) was obtained at 25 ± 2 °C by exposing 100 ppm NO_2 gas. The relationship between response and NO_2 gas concentration of 30% CSA doped PPy/a-Fe2O3 hybrid nanocomposite films is shown in Fig. 6.22. The CSA doped PPy/a-Fe2O3 nanocomposites demonstrated a better response, stability and shorter recovery times as compared to PPy and PPy/a-Fe_2O_3 nanocomposites alone. Therefore, PPy/a-Fe_2O_3 is considered as an excellent gas sensor at room temperature which could be used for selective detection of NO_2 sensors. PANI based nanocomposite ion-exchange materials and their sensing applications is shown in Table 6.1.

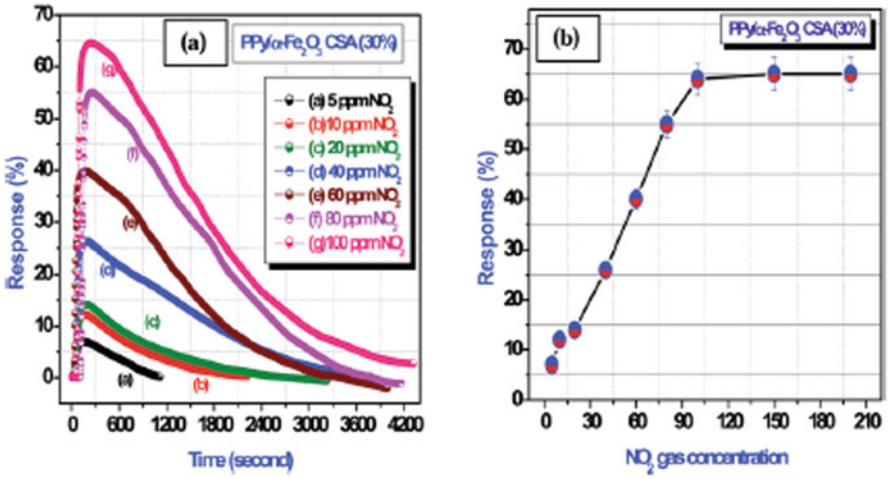

Fig. 6.22 (**a**) Response to 30% CSA doped PPy/a-Fe_2O_3 thin film for various concentrations of NO_2 gas and (**b**) relationship between response and NO_2 gas concentration to 30% CSA doped PPy/a-Fe_2O_3 thin film. (Reprinted with permission, Navale et al. 2014)

6.3 PANI Based Nanocomposites and Their Sensing Applications in Diverse Fields

6.3.1 Detection of Volatile Organic Compounds (VOC)

A number of volatile organic compounds (VOC) have a wide range of applications which are generally used in the form of solvents, preservatives and antiseptics and fuels. However, their inhalations (in the form of vapour) have serious health effects. In this regards, detection of alcohol vapours using PANI-metal oxide based inclusions PANI-Pd nanocomposite has been synthesized (Athawale et al. 2006). The material was used for the sensing behaviour of methanol, and the results revealed that nanocomposite material covered a very high sensing response (~10^4 magnitudes) towards the equilibrium level of methanol. FTIR analysis confirmed the inclusions of Pd in the matrix of PANI which act as a catalyst for reduction of imine nitrogen by methanol. However, in a mixture of VOCs, the PANI-Pd nanocomposite selectively detected methanol with an identical magnitude of response which covered longer response time.

Choudhury et al., fabricated Ag nanoparticles embedded in the matrix of PANI for the detection of ethanol (Choudhury 2009). Nanocomposite materials demonstrated more rapidly protonation–deprotonation responses as compared to pure PANI. In addition, PANI-Ag based nanoparticle have also been used for the sensing behaviour of toluene and triethylamine (Li et al. 2013a). Sensing responses of the material was investigated regarding chemisorption and diffusion mode.

Table 6.1 Some reported PANI based nanocomposite ion-exchange materials

S. no	Nanocomposite	Analysis	Application	References
1.	Polyaniline–titanium(IV)phosphate	FTIR, SEM, TEM, TGA	Sensing of ammonia	Khan et al. (2011)
2.	PANI–TiP	FTIR, XRD, SEM, TGA	Sensing of methanol	Khan et al. (2010b)
3.	V_2O_5@polyaniline nanofiber	SEM, TEM, XRD, TGA-DTA-DSC, XPS, UV–vis.	Sensing of ammonia	Hasan et al. (2015)
4.	P3MTh–TMP	FTIR, SEM, TEM, XRD, TGA	Sensing of ammonia	Khan and Baig (2013a)
5.	PANI/WO_3/GR/GCE	CVs, SWVs, XRD, AFM, Raman spectroscopy, EIS, HRTEM, FTIR	Phenanthrene	Tovide et al. (2014)
6.	Ppy/ZSI	FTIR, XRD, SEM, TEM, EDX,TGA	Formaldehyde	Khan et al. (2013a)
7.	POT-TiP	TEM, XRD, SEM, FTIR	Humidity	Khan and Baig (2013b)
8.	POA-SAP	SEM, TEM, XRD, TGA-DTA	Humidity	Khan et al. (2013b)
9.	PANI-TMP	FTIR, SEM, TEM, XRD, TGA, UV-Vis.	Methanol, ethanol, 1-propanol	Khan et al. (2013a)
10.	PANI-ZSM-5	FTIR, SEM, TEM, XRD	epinephrine, paracetamol, and folic acid	Kaur and Srivastava (2015)
11.	Pani@MWCNT	FTIR, XRD, Raman spectroscopy, SEM, and TEM	Ammonia	Ansari et al. (2014)
12.	PANI/MWCNTs	UV–vis., FT-IR, Raman Spectroscopy, XRD, XPS, HRTEM	Ammonia	Abdulla et al. (2015)
13.	LDH/PANI	UV–vis., SEM, AFM	Ammonia	Xu et al. (2013a)
14.	PANI/TiO_2	SEM,	Ammonia, CO	Tai et al. (2007)
15.	PmAP/c-MWCNT	FTIR, XRD, SEM, TEM	Alcohol	Verma et al. (2015)
16.	PANI/In_2O_3	SEM, TEM, XRD	H_2, CO, NO_2	Sadek et al. (2006)
17.	PHTh, PEDT, PHTh–PEDT/SnO_2	UV, FTIR	NO_2	Ram et al. (2005a)
18.	PANI/Mn_3O_4	–	Humidity	Singla et al. (2007)
19.	Ti–PTFE	SEM, AFM, XPS	Volatile organic compound	Rujisamphan et al. (2016)
20.	PCL-g-CNT	NMR, SEM, AFM	Water, methanol, toluene	Castro et al. (2009)
21.	PANI-WO_3	FTIR, SEM, TEM	CO_2	Chaudhary and Kaur (2015)
22.	PPy/a-Fe_2O_3	XRD, FESEM, TEM	NO_2	Navale et al. (2014)

Nanomaterial showed sensing responses towards triethylamine and toluene, however, deprotonation of PANI and swelling of the polymer results drop in its sensitivity.

Chloroform is an anaesthetic widely used solvent and its inhalation cause depression of the central nervous system. The monitoring of chloroform was reported by the synthesis of PANI-Cu nanocomposite (Sharma et al. 2002). An adsorption–desorption mechanism was adequately described at the surface of metal clusters. The FTIR analysis established interaction of chloroform with metal clusters of the composite. It was observed that PANI supported PANI-Cu demonstrated excellent performance in the detection of chloroform.

Besides the detection of methanol, ethanol, and chloroform, PANI based nanomaterials have also been used as sensors for the detection of reducing gases, namely NH_3 and H_2S which generally depend on deprotonation of PANI. Deprotonation of PANI was achieved by exposing reducing gases through electron donation which result in the enhancement of PANI resistance. However, the addition of metal impurity improves the sensitivity of the sensor. Detection of gases using PANI supported metal oxide nanocomposite have been extensively studied. It was found that addition of metal with PANI forms a p-n heterojunction with a depletion layer. Owing to the formation of the depletion region, nanocomposite materials demonstrated adsorption of gases in the form of alternation in electrical responses. The change in electrical conductivity of nanocomposites altered its sensing behaviour of nanocomposite towards the gases. Thus, PANI-TiO_2 nanocomposite was fabricated by spin coating technique for detection of NH_3. Nanocomposite sensor was examined by using different concentrations of NH_3 (Pawar et al. 2011). The thin film of nanocomposite sensor exhibited good sensing response towards NH_3 below 20 ppm. Sensing characteristic of the sensor was occurred due to the formation of a positively charged depletion layer at the heterojunction of PANI and TiO_2. On increasing concentration of NH_3, the gas sensing response and recovery time increases simultaneously while response time shows opposite behavior. XRD pattern of PANI changes the morphology of nanocomposite as amorphous nature after addition of PANI. XRD diffraction pattern shows sharp and well defined peaks which confirmed the crystalline nature of nanocomposite as shown in Fig. 6.23.

The SEM image of the PANI film demonstrated fibrous morphology with many pores and gaps among the fibers that covered an average grain size of about 60 nm. The image of the nanocomposite (Fig. 6.24c) exhibits no agglomeration of particle and a uniform distribution of the TiO_2 particles in the matrix of PANI which established that the particle of TiO_2 is embedded within the netlike structure built by PANI chains (Fig. 6.24).

A similar finding for the detection of NH_3 reported by Dhingra et al. (2013). However, a different observation was reported by Deshpande and coworkers who studied the response of PANI-SnO_2 nanocomposite towards NH_3 (Deshpande et al. 2009). They observed that pure PANI was found to be reduced in the absence of NH_3 while the nanocomposite showed an oxidative in the presence of NH_3. The I–V characteristic of the nanocomposite, shown in Fig. 6.25c, revealed a diode-like character associated with electrical conductance through the hopping mechanism. Due to the existence of n-type SnO_2 in the matrix of PANI, the formation of

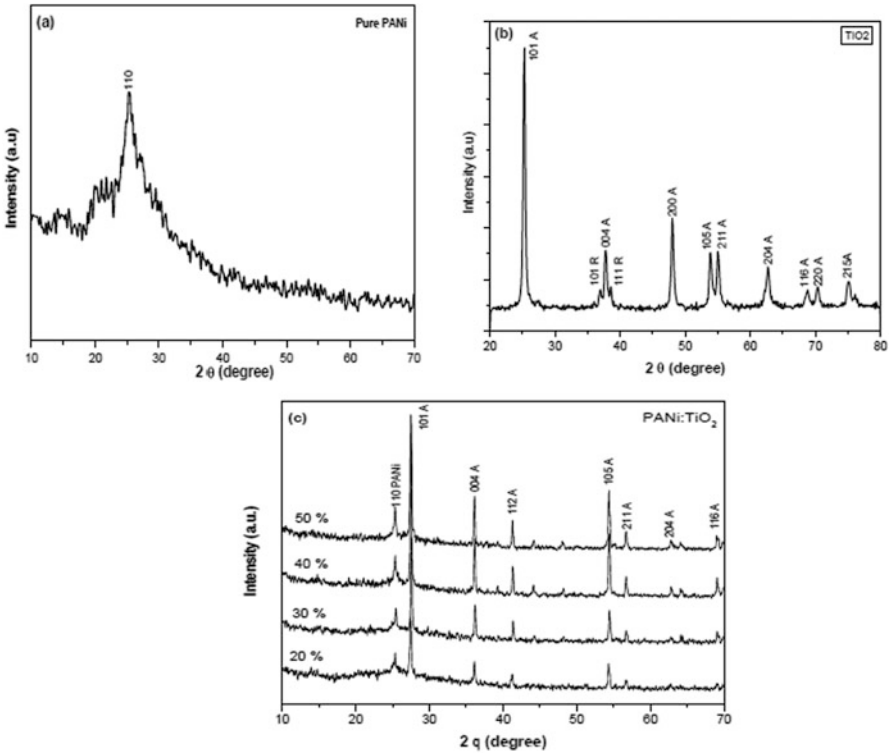

Fig. 6.23 X-ray diffraction patterns of Pure PANi (**a**), TiO_2 (**b**) and PANi/TiO_2 (0–50 wt) (**c**). (Reprinted with permission, Pawar et al. 2011)

localized p–n heterojunction carried out which make PANI-SnO_2 nanocomposite electrically more insulator. Exposure to NH_3 gas resulted in polarization of NH_3 molecules by the depletion region, which provided positive charge on the surface of PANI and the mobility of these charges along the PANI chain made the nanocomposite relatively more conducting. Thus, the formation of p–n heterojunction between PANI and nano-metal oxide plays an essential role as reported by other researchers (Patil et al. 2011; Khuspe et al. 2013).

Aligned poly(methyl methacrylate) (PMMA) fibers were synthesized via electrospinning, and the chain of PANI was grown on the surface of the PMMA fibers to develop PANI/PMMA nanocomposite (Zhang et al. 2014). PANI/PMMA nanocomposite was employed for trace level detection of NH_3 in the concentration as low as 1 ppm. Morphology of PANI/PMMA composite was examined by SEM and Raman spectrometry. Sensing behaviour study revealed that arranged fibers of PANI/PMMA exhibited high sensitivity and fast response upon exposure to ammonia vapor of 1–30 ppm. The high sensitivity response of nanocomposite was accredited due to the highly aligned PMMA microfibers coated with PANI which facilitated faster diffusion of gas molecules, thereby, accelerating electron transfer.

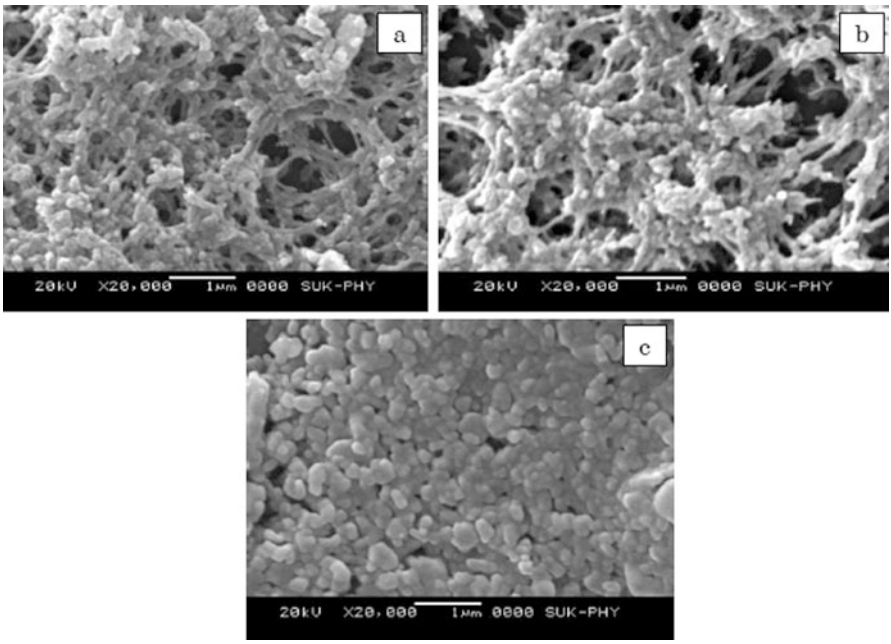

Fig. 6.24 Scanning electron micrographs of (**a**) PANi, (**b**) TiO_2 and (**c**) PANi/TiO_2 (50 wt) films. (Reprinted with permission, Pawar et al. 2011)

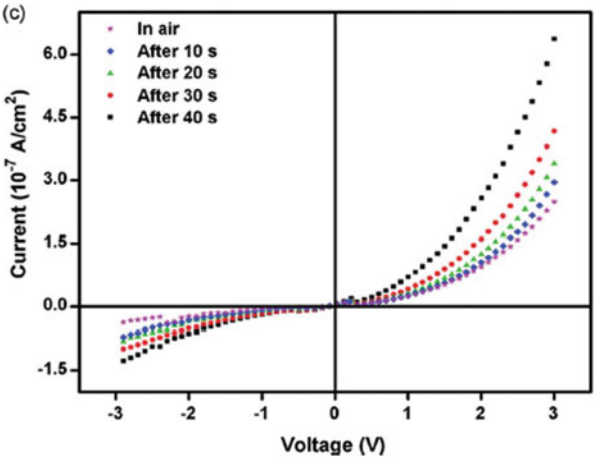

Fig. 6.25 I–V curves (in the presence of ammonia gas) (c) tin oxide/ polyaniline nanocomposites. (Reprinted with permission, Deshpande et al. 2009)

Another porous thin film nanocomposite of PANI/sulphonated Ni phthalocyanine (PANI-NiTSPc) was fabricated for the detection of NH_3 gas (Zhihua et al. 2016). Ammonia gas-sensing behaviour of nanocomposite films was examined under optimum conditions at room temperature. The observed response value (S) of the composite film up to 100 ppm NH_3 was found as 2.75 in short response time (10 s).

Over a concentration range of 5–2500 ppm, PANI/NiTSPc films demonstrated a fast recovery rate, good reproducibility, and acceptable long-term stability. The outstanding sensing performance was achieved because of porous, ultra-thin film structure and the "NH_3-capture" effect of the "flickering" NiTSPc molecules. Thus, the proposed PANI-NiTSPc nanocomposite thin film sensors were found to be excellent potential candidates for the detection of NH_3.

Crowley and co-workers synthesized PANI-$CuCl_2$ nanocomposites sensor printed on screen printed interdigitated electrodes for the detection of H_2S gas at trace level (Crowley et al. 2010). The sensing material was composed of screen printed silver interdigitated electrode (IDE) on a flexible PET substrate along with inkjet printed layers of PANI and copper (II) chloride. The finding of sensing behaviour explored a different phenomenon in which protonation of PANI nanocomposite occurred during the exposure of H_2S gas. It was found that PANI gets deprotonated by complexation of $CuCl_2$ due to binding of $CuCl_2$ with S^{2-} ion caused the evolution of HCl which improved the electrical conductivity of PANI. On exposure to hydrogen sulphide; 2.5 ppmv (ppm by volume), nanocompoite sensor showed a linear relationship between measured current and concentration over 10–100 ppmv region. Thus, PANI-$CuCl_2$ based sensor act as chemiresistor concerning measured current and concentration. Sarfraz et al. also reported a similar study based on the synthesis of PANI-$CuCl_2$ nanocomposite printed on interdigitated electrodes for H_2S detection (Sarfraz et al. 2013). Raut and co-workers described the synthesis of PANI based PANI–CdS nanocomposite film by a simple spin coating technique and its application for detection of H_2S gas. Nanocompoite sensor achieved a maximum response (~48%) for 100 ppm H_2S concentration. It was also mentioned that the sensing mechanism of the nanocomposite was achieved by the modifications in nanocomposite at the depletion region (Raut et al. 2012).

PANI based PANI-Au nanoparticles nanowires with a diameter of 250–320 nm had synthesized via electrochemical technique (a two step galvanostatic technique). PANI nanowires were then electrochemically functionalized with gold nanoparticles using cyclic voltammetry technique. Prepared nanocomposite sensor was examined for detection of H_2S gas and fast selective, gas response was observed at room temperature. Proposed mechanism for the formation of AuS and subsequent protonation of PANI for H_2S detection by PANI-Au nanocomposites is given by Eq. 6.1).

$$H_2S + Au/AuS + 2H^+ \tag{6.1}$$

It was suggested that donation of electrons to the protons is followed by the reaction Eq. 6.1) which led to the alternation in the resistance of the PANI-Au nanocomposite. The sensing response of PANI-Au nanocomposite and PANI as a function of time towards different concentrations of H_2S gas is shown in Fig. 6.26. These chemiresistive sensors show an excellent limit of detection (0.1 ppb) along with excellent selectivity and reproducibility over a wide dynamic range (0.1–100 ppb).

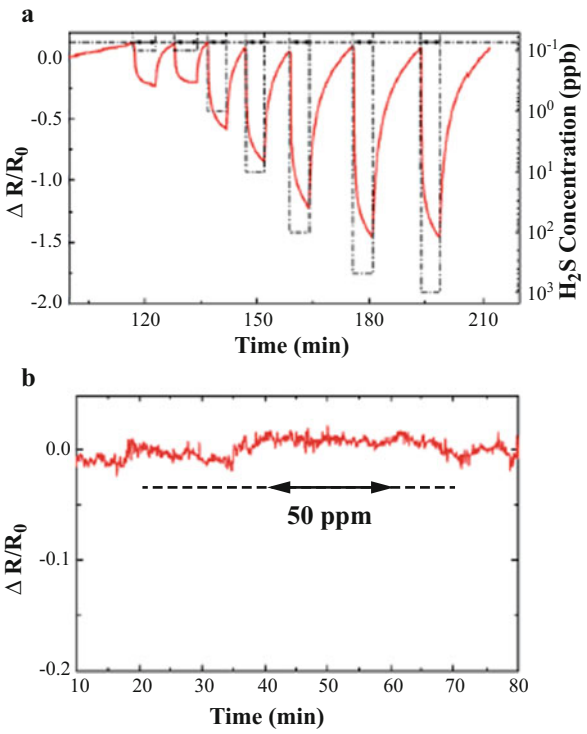

Fig. 6.26 (**a**) Response and recovery transients (solid line) of gold nanoparticles functionalized PANI nanowire network based chemiresistive sensor toward 0.1 ppb, 1 ppb, 10 ppb, 100 ppb, 500 ppb, and 1 ppm (dashed line) concentrations of H_2S gas, (**b**) response of unfunctionalized PANI nanowire network toward 50 ppm of H_2S gas (–- indicates carrier gas and 4 indicates gas analyte) (reprinted with permission) (Shirsat et al. 2009)

6.3.2 LPG Sensing Application

PANI based nanocomposite materials play vital role for safety purposes in the detection of LPG sensing (Joshi et al. 2007). The use of electroactive PANI as a physical transducer at room temperature sensing provides a safer option as opposed to metal oxide based high temperature detectors. In this regard, synthesis of n-CdSe/p-PANI nanocomposite was carried out by a simple electrodeposition technique to examine its sensing response towards LPG. The junction diode was tested to detect the sensitivity of liquefied petroleum gas (LPG) at 25 ± 2 °C. Biased current–voltage characteristics of the junction diode demonstrated a considerable shift by exposing different concentrations of LPG. Nanocomposite sensor showed maximum response up to 70% for 0.08% (by volume) LPG. On the basis of LPG concentration, the response time was found in between the range of 50 and 100 s, while optimal recovery was achieved in 200 s.

A similar finding was reported by the fabrication of PANI/g-Fe_2O_3 nanocomposite to detect sensing of LPG at room temperature (Sen et al. 2014). The nanocomposite films were examined for their response to LPG in the concentration range 50–200 ppm. Morphological characterization was performed by FTIR, UV-vis. XRD, FESEM analyses. The nanoscale morphology of the composites provided a large surface area which enhance the gas sensitivity resulting adsorption

of gas molecules,. The sensing mechanism alters the depletion region of the p–n junction between PANI and γ-Fe_2O_3 which result in an electronic charge transfer between the gas molecules and nanocomposite sensor and optimum responses were obtained for 200 ppm LPG together with response times as low as 60 s. Thus, on the basis of above mentioned observations detection of LPG increase in the depletion depth owing to the adsorption of gas molecules at the depletion region of the p–n heterojunction.

A series of PANI based nanocomposite sensors were fabricated by Dhawale and co-workers (Dhawale et al. 2008, 2010a, b). The materials were used for the sensing responses of LPG at room temperature which demonstrated significant selectivity towards LPG as compared to N_2 and CO_2. The improvement in gas sensing response was found due to a change in the barrier potential of nanocomposite heterojunction.

6.3.3 Sensing Behaviour Towards Humidity

Water vapour plays essential role in the electrical conductance of PANI. Therefore a number of PANI supported nanocomposite were fabricated for the sensing behaviour of humidity (Shukla et al. 2012). PANI-ZnO based nanocomposite electrochemical humidity sensor was developed by the wet-chemical method at ambient condition. The nanocomposite sensor (~200 nm thickness) was examined for the sensing of humidity. The results of sensing study revealed that the particle crystalline homogenous ZnO existed in the matrix of PANI which enhanced electrical conductance in the range of 10^{-2} scm^{-1} and covered thermal stability up to 280 °C. The response and recovery time of the sensor was found between 32 and 45 s, respectively which demonstrated better sensing characteristics than pure PANI and other reported humidity sensors. The adsorption of water molecules on the sensor results in efficient directional charge conduction at the heterojunction formed between PANI and ZnO. Another PANI based humidity sensor of nanostructure Co dispersed in polyaniline deposited as a clad; PANI-Co was reported to determine humidity (Vijayan et al. 2008). The sensor exhibited the quick response of 8 s (20–95% RH) and recovery time in 1 min (95–20% RH) on fibre optical waveguide (in the range of 20–100% RH). In another study, PANI-Ag nanocomposite sensor was developed on an optical fiber clad to examine humidity (Vijayan et al. 2008). The sensing behaviour of PANI-Ag was observed in the range of 5–95% relative humidity (RH). It demonstrated sensing response of humidity with complete reversible nature having almost 1% of standard deviation. Response time of the sensor was found in very short period (30 s) and recovery was achieved in 90 s. By decreasing size of nanoparticles, the improvement in the sensor responses was occurred. Such high responses towards humidity have also been observed with other PANI based nanocomposites as well (Parvatikar et al. 2006; Sajjan et al. 2013).

A fast, responsive humidity sensor was designed by the synthesis of silver vanadium oxide nanospheres dispersed in different ultrathin layers of polyaniline (PANI–β-$AgVO_3$) using in-situ oxidative polymerization (Diggikar et al. 2013). The XRD analysis showed a monoclinic crystallographic form of silver vanadium oxide

(SVO) which was dispersed in ultrathin layers of PANI. Morphological characterization was carried out by FESEM, HRTEM, and AFM analyses. FTIR and EDAX spectroscopic investigations confirmed the existence of SVO in the PANI layer. The SVO dispersed in a layer of PANI-NC revealed excellent humidity sensing characteristics. The response and recovery times are found to be 4 and 8 s, respectively. Cavallo and coworkers demonstrated a high level of relative humidity (65–90%) swelling of the polymer due to continuous absorption of water. The sensing property of PANI increased due to its inter chain distance thus, hindering the charge hopping process and decreasing electrical conductance. It is, therefore, imperative that the influence of humidity on the electrical behaviour of PANI and its pathways be investigated (Cavallo et al. 2015).

6.3.4 Analysis of Miscellaneous Gases

PANI also shows low sensitivity towards certain gasses; methane (CH_4) and carbon monoxide (CO), because these gases do not show redox properties at room temperature (Yan et al. 2009). These analytes may not undergo chemical reactions with PANI, however, have weak physical interaction with the matrix of the polymer. The existence of metal/metal oxide nanoparticles in the matrix of PANI improved its sensing response towards these gases. Polyaniline/Indium(III) Oxide (PANi/In_2O_3) nanocomposite thin films was synthesized and fabricated on AT-Cut quartz crystal microbalance (QCM) of Ag electrodes by the combining two techniques (electrostatic self-assembly and in-situ oxidation polymerization) at 10 °C. The material was used for sensing the study of CH_4 and CO gases. The observed results revealed that PANi/In_2O_3 thin film gas sensor demonstrated good linear sensitivity towards CH_4 and CO, while higher sensing behaviour was achieved for CH_4, (i.e., the sensitivity is 0.386 Hz per ppm when the sensor is exposed to 500 ppm CH_4 while only 0.16 Hz per ppm).

Ram et al. have also proposed theory regarding sensing behaviour of gases detection via catalytic pathway for the detection of CO by PANI-SnO_2 nanocomposite (Ram et al. 2005b). Other PANI-SWCNT nanocomposite based sensor was also synthesized which exhibited good sensing response towards CO (Kim et al. 2010). The mobility of these positive charges generated on the amine nitrogen of PANI increases its conductivity. As compared to NH_3 gas which was also included in the study, the sensor showed a propensity towards CO absorption. In most cases, detection of CO by PANI nanocomposite was described using the particle electron transfer model – the stable resonance structure of $^{+}C{=}O^{-}$ withdraws the lone pair of an electron from the amine nitrogen in PANI thus, creating a positive charge on it. The mobility of these positive charges generated on the amine nitrogen of PANI increases its conductivity.

The highly sensitive and rapid NO gas sensor polyaniline/TiO_2/carbon nanotube composites (PANI-TiO_2-MWCNT) was synthesized (Yun et al. 2013). It was used for NO detection through the photocatalytic behaviour of TiO_2. The gas sensing property of nanocomposite was measured by the changing of electrical resistance

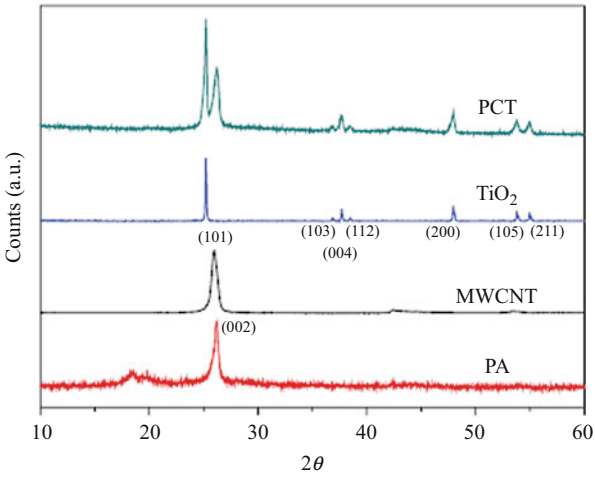

Fig. 6.27 XRD patterns of the prepared samples. (Reprinted with permission, Yun et al. 2013)

without or with UV irradiation for the photo-degradation of NO. The photo-degraded products such as HNO_2, NO_2, and HNO_3, were adsorbed on the PANI-coated carbon nanotubes, resulted decline in electrical resistance due to the p-type semiconductors of carbon nanotube and polyaniline. The XRD pattern of TiO_2 exhibited the characteristics of anatase TiO_2 phase with a tetragonal structure which possessed the photocatalytic properties as shown in Fig. 6.27. Morphological characterization was carried out by FE-SEM analysis. The FE-SEM images of nanocomposite show aggregated PANI phases of the uniform sized spherical type. The average size of PANI spherical phases was measured as 193 ± 27 nm (average value measured five times). The uniformly coated PANI on MWCNTs has observed with the average thickness of the PANI coating layer was around 23 ± 8 nm considering the average diameter of MWCNTs (130 ± 15 nm). PANI was also coated on TiO_2 particles; it was aggregated to some extent as shown in Fig. 6.28c. PCT sample showed the TiO_2 particles dispersed on the PANI-coated MWCNTs as shown in Fig. 6.28d. It was examined that under UV irradiation, the NO gas gets decomposed by the photocatalytic effect of TiO_2 resulted HNO_2, NO_2, and HNO_3. These decomposition products adsorbed onto the surface of PANI/MWCNT owing to its high specific surface area and hydrophilicity of PANI. Such combining effects alter the electrical resistance of the nanocomposite, thus, facilitating detection. Figure 6.29 shows the sensitivities (S) of the nanocomposites towards NO under UV irradiation. PANI/TiO_2/MWCNT nanocomposite (PCT) exhibited a high response of NO, while PANI (PA) showed the least. PANI-MWCNT (PC) and PANI-TiO_2 (PT) composites showed better response as compared to its components.

PANI has also been used for the detection of a number of gases including NO_2 and H_2 supported nanocomposites (Xu et al. 2013b; Srivastava et al. 2010). Introduction of CNT or metal oxides into PANI have shown response towards H_2 gas. Interdigitated electrodes based on PANI-TiO_2 and PANI/MWCNTs were used for the detection of H_2 gas with both of the nanocomposite materials demonstrated eliciting a high sensing response.

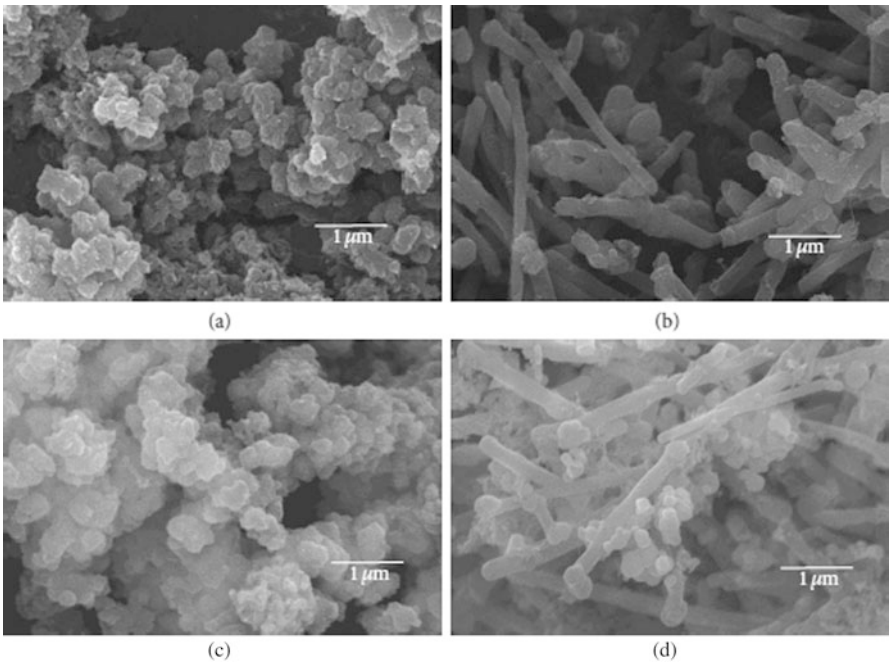

Fig. 6.28 FE-SEM images of (**a**) PA, (**b**) PC, (**c**) PT, and (**d**) PCT samples. (Reprinted with permission, Yun et al. 2013)

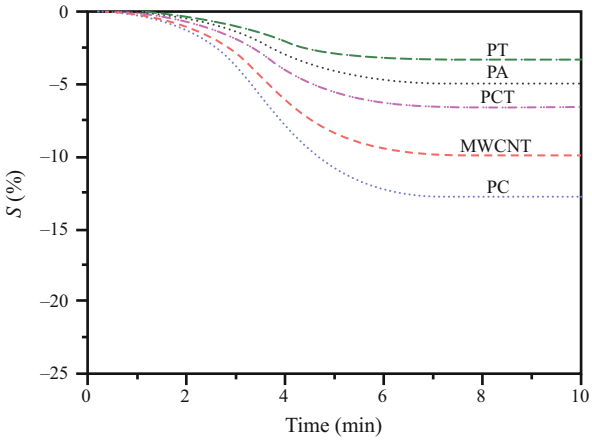

Fig. 6.29 NO gas sensing behaviour of various samples under UV irradiation. (Reprinted with permission, Yun et al. 2013)

The structural characterization and gas sensing behaviour of PANI-MWCNTs based surface acoustic wave (SAW) sensor deposited on lithium tantalite SAW transducers for H_2 gas was also reported (Arsat et al. 2011). The SEM analysis explored the dense growth of nanocomposite which was much denser than that of PANI nanofibers. Another SAW based PANI-WO_3 sensor deposited on layered

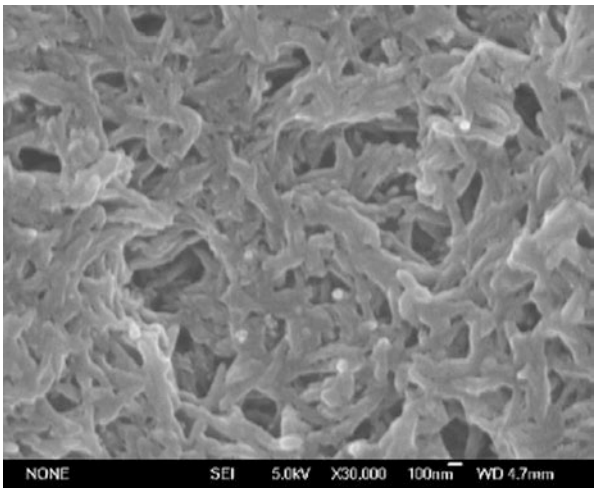

Fig. 6.30 SEM image of polyaniline/WO3 nanofibers. (Reprinted with permission, Sadek et al. 2008)

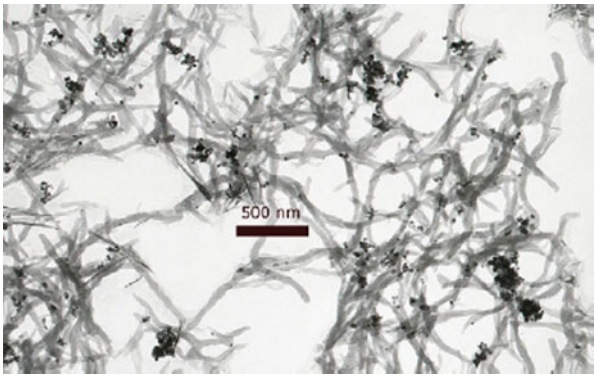

Fig. 6.31 TEM image of polyaniline/WO3 nanofiber composite. (Reprinted with permission, Sadek et al. 2008)

ZnO/64° YX $LiNbO_3$ SAW transducer using oxidative chemical polymerization which showed fast sensing response together with good repeatability (Sadek et al. 2008). XRD, SEM and TEM analyses characterized it. The average of the PANI-WO_3 nanofiber layer on the substrate measured by profilemeter was found as 0.4 nm. The average diameter of the nanofibers was 90 nm and shows a connecting network with each other (Fig. 6.30). Nanoparticles of WO_3 embedded in the backbone of PANI (Fig. 6.31). TEM image shows the embedded WO_3 nanoparticles are integrated into the polyaniline nanofibers backbone. From SEM and TEM images, it can be concluded that the deposited thin film is porous. SEM and TEM analyses confirmed the porous nature of PANI-WO_3 nanocomposite. The XRD shows sharp line-peaks in the bottom which confirmed the existence of WO_3 (from JCPDS database) in the matrix of PANI and the peaks in the above are due to the PANI-WO_3 nanocomposite (Fig. 6.32).

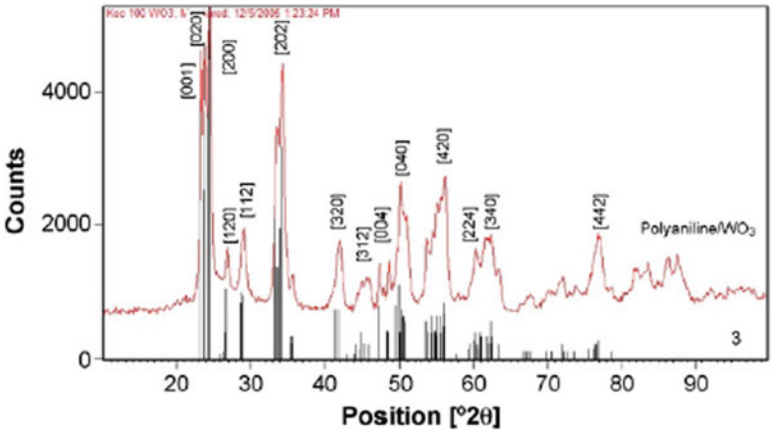

Fig. 6.32 XRD image of polyaniline/WO3 nanofiber composite. (Reprinted with permission, Sadek et al. 2008)

A PANI-PtO_2 based thin film sensor has also been reported for H_2 sensing (Conn et al. 1998). The authors stated that during the exposure of H_2 gas under the sensing condition, the PtO_2 present in the matrix of PANI was reduced to PtO. It catalytically oxidizes to water which decreases the resistance of PANI.

An interdigitated electrode of PANI–chloroaluminium phthalocyanine (PANI-ClAlPc) for CO_2 detection has been prepared by spin coating method from PANI as the base of composites and ClAlPc (with different concentrations) as the second component (Azim-Araghi and Jafari 2010). To determine the sensitivity, reversibility, response and recovery time, these nanocomposite thin films were exposure to different concentrations (0–2000 ppm) of CO_2 gas. For the practical application, the composites sensors were investigated at different temperatures. The sensitivity factor of composites has covered a range between 0.05–7.20. An optimum concentration of 10% ClAlPc was chosen in the matrix of PANI for maximum sensitivity at 300 K. Nanocomposite sensor demonstrated unexpected behaviour and the conductivity of thin films that was increased on exposure lower RH % and decreased on higher RH %. The results of sensing behaviour confirmed that the CO_2 mixtures reduced the sensitivity of thin films in compression with pure CO_2 (1000 ppm).

The sensing of gas can perform using different pathways – from nanometal catalyzed reaction to modification of barrier height. The response extracted from a nanocomposite sensor on exposure to an analyte (gas) generally governed: (i) charge transfer phenomenon between the constituents of the nanocomposite, and (ii) reaction between the gas and the nanocomposite. For example, H_2S can either have a reducing or an oxidizing effect on PANI depending on the interaction of PANI with the secondary component in the nanocomposite. Moreover, taking into consideration, the humidity factor is found necessary because it significantly decreases the sensitivity of PANI sensors. Therefore, for future PANI based sensing materials, a deeper understanding of the sensing behaviour is required to develop high performance sensors.

6.3.5 PANI Based Biosensors Nanocomposites

Biosensor system which functioned through immobilized sensor activity was first time reported by Lowe (Lowe 1984). It was the beginning of modern biosensors that has been widely used in nowadays. Their system comprised of an enzyme (glucose oxidase) immobilized on a gel which measured the concentration of glucose in biological solutions. A number of biosensors have come up since, which find finding applications in various fields including; industry, clinical diagnostics and environment monitoring (Baraton 2008).

A biosensor typically consists of a biorecognition element (or bioreceptor), a transducer element, and electronic components for signal processing. The schematic of a biosensor operation is shown in Fig. 6.33. It operates in three stages – (i) recognition of a specific analyte (gas) by the bioreceptor, (ii) transformation of biochemical reaction into the transducer-type reaction, and (iii) processing of transducer signal (Baraton 2008).

The enzyme based electrode is a miniature chemical transducer which functions by combining an electrochemical procedure with immobilized enzyme activity. This particular model employed glucose oxidase immobilized on a gel to measure the concentration of glucose in biological solutions as well as in the tissues in vitro.

PANI is particularly attractive as biosensors because it gives a conducting matrix for immobilization of bioreceptors (i.e., confined movement of bioreceptors in a defined space) onto it. Its electroactivity allows it to act as a mediator for electron transfer through a redox or enzymatic reaction. Such direct communication with the bound bioreceptors leads to a range of analytical signals which provides a measurement of the sensor activity (Dhand et al. 2011). This conducting polymer showed

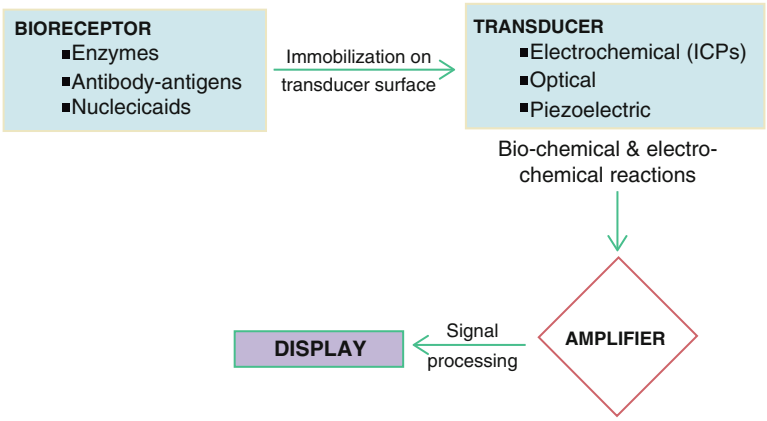

Fig. 6.33 Schematic representation of biosensor operation. (Reprinted with permission, Baraton 2008)

significant binding capacity with biomolecules along with fast electron transfer to produce new analytical applications. Apart from its electronic properties, PANI has shown excellent stability and strong biomolecular interactions (Di and Ivaska 2006; Imisides et al. 1996) that is found necessary for biosensor applications. On the basis of electrical conductivity, electrochromism, and pH sensitivity PANI has been successfully used for detection of different biological compounds (Muhammad-Tahir and Alocilja 2003; Malinauskas et al. 2004; Hoa et al. 1992). PANI based nanocomposite materials provide a scope to further assess their potential as biosensors. A secondary component in the matrix of PANI is often seen to increase bioreceptor binding onto PANI surface. Based on the response of bioreceptors, biosensors are broadly classified as enzymatic biosensors, immunosensors, and DNA/nucleic acid biosensors:

6.3.5.1 Enzymatic Biosensors

Clark and Lyons has introduced the concept of enzymatic biosensors by using the enzyme glucose oxidase (GOx) (Clark and Lyons 1962). An amperometric biosensor was developed in which the enzyme catalyzed the oxidation of glucose on the surface of the Pt electrode. Because of the enzymatic reaction, the oxygen flux on electrode surface varied as a function of glucose concentration, thus enabling its detection. However, the enzyme activity carried out in solution as opposed to the recent biosensors which have immobilized enzymes.

6.3.5.2 Glucose Biosensor

The biosensor of glucose was first introduced by significant modifications with reference to its detection technique and development of newer materials for enzyme immobilization. A novel glucose biosensor based on a composite of Au nanoparticles (NPs)–conductive polyaniline (PANI) nanofibers (PANI-Au) has been synthesized by Xian et al. (Xian et al. 2006). Nanocomposite material was immobilized with glucose oxidase (GOx) and Nafion on the surface by electrochemical oxidation of H_2O_2. It was found that the PANI-Au nanocomposite observed a much higher anodic current as compared to pure PANI. This resulted a better response, possibly due to fast electron transfer between electrode and H_2O_2 facilitated by Au in PANI matrix. It demonstrated a linear calibration curve over the concentration range from 1.0×10^{-6} to 8.0×10^{-4} mol/L, with a slope and detection limit (S/N = 3) of 2.3 mA/M and 5.0×10^{-7} M, respectively. In addition, the glucose biosensor system indicates excellent reproducibility (less than 5% R.S.D.) and good operational stability (over 2 weeks).

Other PANI based PANI/MWCNTs nanocomposites have also been reported, and these were used as biosensors for the detection of glucose (Gopalan et al. 2009; Zhong et al. 2011; Fu and Yu 2014). A novel glucose biosensor was developed based on the direct electrochemistry of glucose oxidase (GOD) adsorbed in graphene/polyaniline/gold nanoparticles (AuNPs) nanocomposite modified glassy carbon electrode (GCE) (Fu and Yu 2014). In comparison to graphene, polyanilline (PANI) or graphene/PANI, the graphene/PANI/AuNPs nanocomposite, graphene/PANI/AuNPs was found was more biocompatible and it offered a favourable microenvironment for facilitating the direct electron transfer between GOD and electrode. The adsorbed GOD displayed a pair of well-defined quasi-reversible redox peaks with a formal potential of −0.477 V (vs. SCE) and an apparent electron transfer rate constant (ks) of 4.8 s^{-1} in 0.1 M pH 7.0 PBS solution. The amperometric response of GOD graphene/PANI/AuNPs modified electrode showed improvement in amperometric response with respect the concentration of glucose (in the range of 4.0 M–1.12 mM) at lower detection limit; 0.6 M (at signal-to-noise of 3). Addition of GOD to prepare graphene/PANI/AuNPs nanocomposite showed its selective behavour for detection of glucose. Le et al., developed a PANI/MWCNTs biosensor deposited on interdigitated planar Pt-film electrode over which the GOx was immobilized via glutaraldehyde (Le et al. 2013). The rapid amperometric response of PANI/MWCNTs concerning with the changing in glucose concentration is shown in Fig. 6.28. The porous nature of the nanocomposite facilitated stronger binding to GOx, and the nanocomposite proved to be an efficient transducer with a response time of 5 s. A GOx immobilized PANI–TiO_2 nanotube composite as an electrochemical biosensor reported by Zhu and co-workers (Zhu et al. 2015). Nanocomposite materials demonstrated excellent biocompatibility, better electrical conductivity, low electrochemical interferences and high signal-to-noise ratio for the development of electrochemical biosensors.

TiO_2 nanoparticles were initially transformed into TNTs, on which aniline was polymerized by oxidative polymerization to form an intimate and uniform PANI–TNT composite using a hydrothermal method. Characterization of the nanocomposite was carried out by different spectroscopic techniques. The PANI–TNT nanocomposite was used to immobilize glucose oxidase (GOD) for the construction of an electrochemical biosensor. Cyclic voltammetry studied the direct electrochemistry, and electro-catalytic performance of the biosensors based on PANI-TNTs and TNTs. The performance studies revealed that the nanoscaled tub-like morphology facilitated direct electron transfer of GOx, giving a sensitivity of 11.4 mA mM1 at a low detection range of 0.5 mM at a high signal-to-noise ratio (Fig. 6.34).

Although most of the biosensors utilize immobilized GOx for the detection of glucose, other enzymes can also be used for this purpose. In this regards, Ozdemir et al., reported a biosensor based on pyranose oxidase immobilized Au/PANI/AgCl/gelatin nanocomposite for glucose detection, wherein sensing was facilitated by amperometric detection of consumed O_2 during the enzymatic reaction (Ozdemir et al. 2010). The importance of glucose biosensors lies in the simpleistic and accurate monitoring of blood glucose levels, which might help in controlling the growing issue of diabetes around the world.

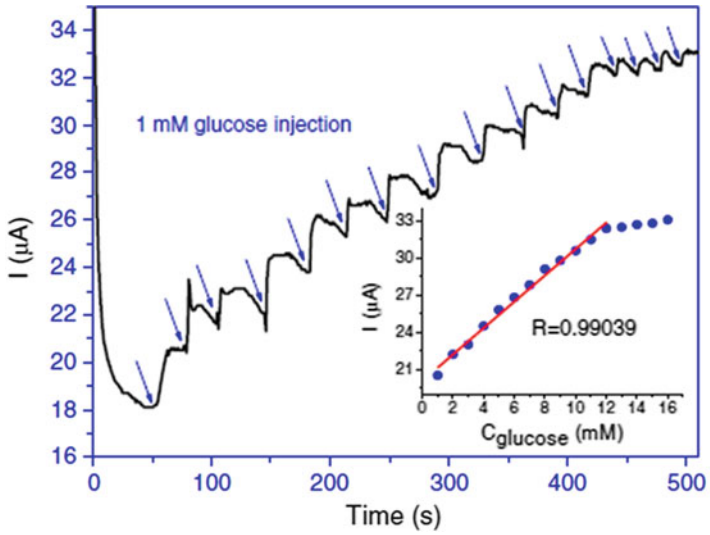

Fig. 6.34 Amperometric response of GOx/PANI-MWCNT/IDmE upon increasing the glucose concentration in steps of 1 mM at +0.6 V (versus SCE) in PBS. The inset shows the calibration plot156 (Reproduced with permission from IOPscience). (Reprinted with permission, Le et al. 2013)

6.3.5.3 PANI Based Immunosensors

Immunosensor is made of the combination of antigen–antibody specificity and transducer forms. For the detection of salbutamol (SAL), an ultrasensitive electrochemical immunosensor based on nanogold particles (nano-Au), Prussian Blue (PB), polyaniline/poly (acrylic acid) (PANI (PAA)) and Au-hybrid graphene nanocomposite (AuGN) was developed by Huang et al., (Huang et al. 2011). Nano-Au, PB, and PANI (PAA)-incorporated film was used to enhance the electroactivity, stability and catalytic activity for hydrogen reduction. AuGN was employed to immobilise chitosan, nano-Au and horseradish peroxidase–anti-SAL antibody (HRP–AAb). The resulting nanostructure (AuGN–HRP–AAb) was used as the label for the immunosensor. A label of chitosan coated graphene with the nano-Au shell was used to immobilize HRP-anti-SAL antibody on this multicomponent nanocomposite. The immunosensor showed excellent catalytic activity for hydrogen reduction on the electrode.

In another study, Liu and co-workers prepared a novel graphene oxide nanosheets/polyaniline (GO/PANI/CdSe) nanowires for detection of interleukin-6 (Liu et al. 2013). The GO/PANi/CdSe nanocomposites demonstrated excellent biocompatibility, dispersity, and solubility. Electrochemiluminescence (ECL) of CdSe quantum dots (QDs) was greatly enhanced by combining with GO/PANi nanocomposites. The nanocomposite of GO/PANi/CdSe was employed to develop an ultrasensitive ECL immunosensor for the detection of IL-6. The nanocomposite showed high specificity, long term stability and reproducibility with a detection limit as low as 0.17 pg mL^{-1}.

Polyaniline nanowires (PANI) and gold nanoparticle (AuNPs) based hybrid nanocomposite film has been fabricated onto an Au substrate. The prepared nanocomposite was used to develop a mediator free immunosensor for the detection of PSA (Dey et al. 2012). Microscopic studies revealed uniform distribution of the AuNPs in the PANI backbone provides desired microenvironment for antibody immobilization. The results of electrochemical studies proposed that AuNPs improve the electro-active surface area of PANI and resulted in high electron transport in a mediator free electrolyte. The sensor performance was measured using differential pulse voltammetry (DPV) which studied the electrochemical changes resulting from the biochemical reactions on the surface. Microscopic studies established a uniform distribution of the AuNPs on the PANI backbone resulting in a nanoporous morphology that provides the desired microenvironment for antibody immobilization. The nanocomposite provided a high surface area for immobilization of anti-PSA, which improved electron transfer and results high performance of the immunosensor. The electrochemical response studies of the immunosensor to different concentrations of PSA are shown in Fig. 6.35. The sensor exhibited good linearity, high sensitivity and excellent response at very low concentrations. The immunosensor showed excellent stability up to 5 weeks after that stability decreases and current response became low.

Synthesized PANI-Au nanoparticles were studied using UV-vis. spectroscopy. The broadening of the observed absorption peak is accredited to the presence of different size particles. It is generally found that Au nanoparticles are known to exhibit a strong surface plasmon absorbance band at about 520 nm which depends on size, shape, material properties, surrounding media, and proximity to other nanoparticles. The particle size of Au nanoparticles was measured at 50 nm using the UV absorbance peak at 535 nm. The particle size, shape, and distribution of the Au nanoparticles were studied using TEM analysis (inset, Fig. 6.36a). TEM images exposed crystalline nature of Au nanoparticles with minimal agglomeration among the particles, and they appear in icosahedra shape with an estimated particle size of ~50 nm. SEM studies (Fig. 6.30) of synthesized PANI (image a) exhibited very smooth surface with a homogenous diameter estimated as 100–200 nm with length varying from 1 to 2 microns. After the electrophoretic deposition of PANI nanowires onto the Au substrate, the SEM study (image b) exhibited the uniform deposition of PANI nanowires over a large surface area without a significant change in length and diameter of the nanowires. The SEM image of the Au-NPs-PANI–Au nanocomposite (image c) depicted that AuNPs are uniformly distributed onto the PANI surface via self-assembly due to differences in surface charges resulting in strong electrostatic interactions. Moreover, AuNPs are dispersed over PANI with minimal agglomeration, which is expected to improve the electrochemical properties of PANI.

A multilayer nanocomposite of Au-PANI-cMWCNTs-chitosan was used to design a highly sensitive immunosensor for detecting an organophosphate insecticide (i.e., chlorpyrifos) (Sun et al. 2013). PANI-coated MWCNTs were fabricated via in-situ oxidative polymerization. Carboxylated MWCNTs played a significant role to achieve the thin and uniform coating of PANI, thus, resulting in the improved

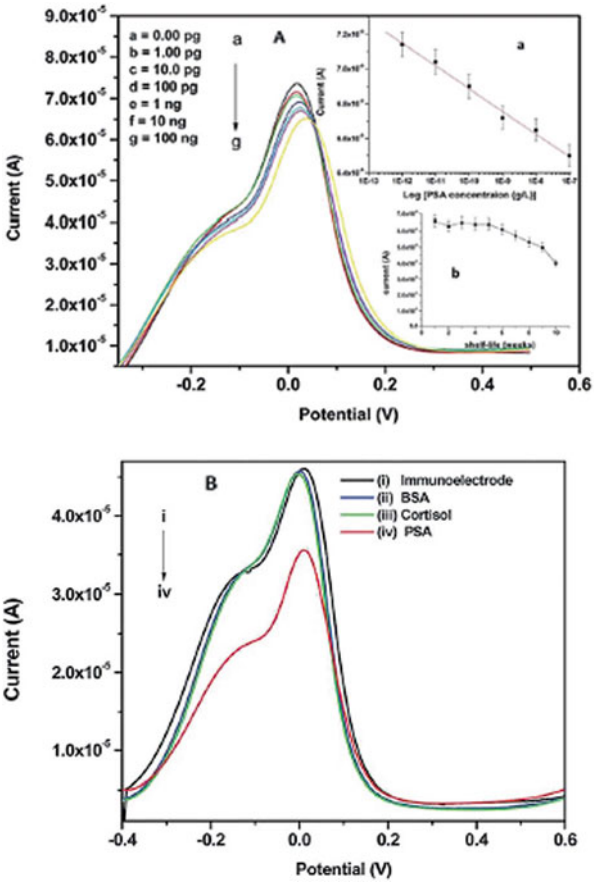

Fig. 6.35 (**A**) Electrochemical response studies of the BSA/anti-PSA/AuNP-PSA/Au immunoelectrode as a function of PSA (1 pg mL1–100 ng mL^{-1}) in PBS (10 mM, pH 7 containing 0.9% NaCl) using DPV technique. Inset (**a**) calibration curve between the magnitude of electrochemical response current vs. logarithm of PSA concentration and inset (**b**) shelf-life studies of BSA/anti-PSA/AuNP-PSA/Au immunoelectrode. (**B**) Interference studies of BSA/anti-PSA/AuNP-PSA/Au immunoelectrode using BSA (10 ng mL^{-1}) and cortisol (10 ng mL^{-1}) concerning with PSA (10 ng mL^{-1}). Reproduced from178 with permission from The Royal Society of Chemistry. (Reprinted with permission, Dey et al. 2012)

immunosensor response. The immunosensor showed higher sensitivity and specific immunoreactions for analysis of real samples as well. Besides, storage at low temperatures affords the sensor a longer shelf life as in case of other biosensors. Experimental parameters affecting the preparation process and analytical performance of the immunosensor were optimized. Under optimal conditions (antibody concentration: 5 μg/mL, working buffer pH: 6.5, incubation time: 40 min, incubation temperature: 25 °C), the immunosensor showed a wide linear range from 0.1 to 40×10^{-6} mg/mL and from 40×10^{-6} mg/mL to 500×10^{-6} mg/mL. The detection limit was found to be 0.06×10^{-6} mg/mL which provided a valuable tool for the chlorpyrifos detection in real samples.

Graphene/PANI nanocomposite (GR–PANI) based immunosensor has been utilized for the detection of estradiol (Li et al. 2013b). GR–PANI composites was used to enhance the electroactivity and stability of the electrode. During the synthesis, Horseradish peroxidase–graphene oxide–antibody (HRP–GO–Ab) conjugates was constructed by using the carboxylated GO (as the carrier of the antibody), resulting

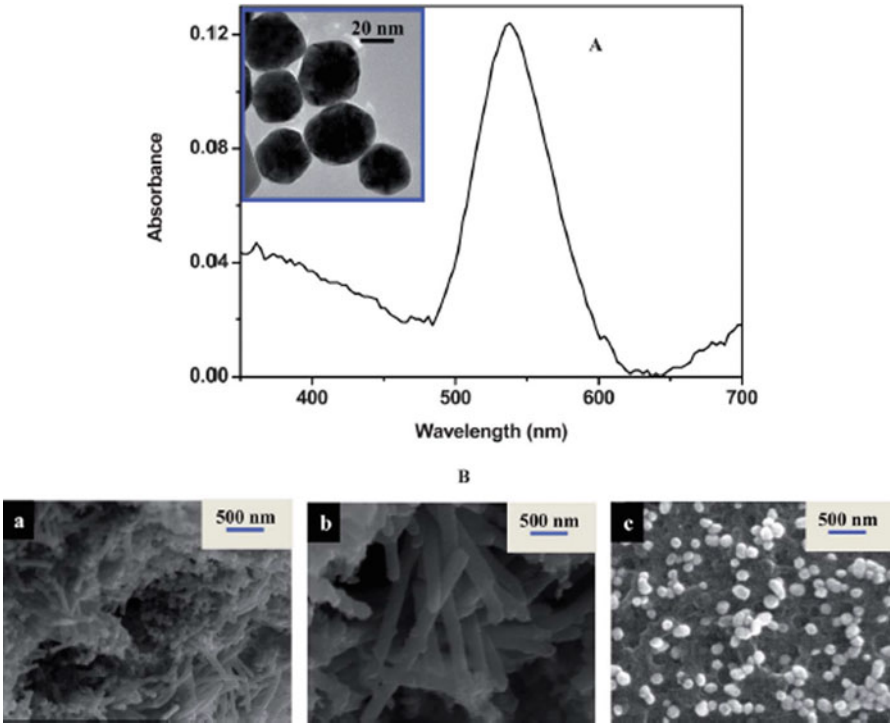

Fig. 6.36 (**a**) UV-visible absorption spectra of AuNPs, (inset) TEM image of AuNPs synthesized by co-precipitation method, (**b**) SEM images of PANI nanowires (image a) prepared by chemical oxidative method, (image b) electrophoretically deposited PANI nanowires onto the Au substrate, (image c) self assembled AuNPs on the nanostructured surface charged PANI/Au electrode. (Reprinted with permission, Dey et al. 2012)

in the improved catalytic activity of the hydrogen reduction of the electrode. The current response of the immunosensor was remarkably enhanced due to the synergistic effects of GR and PANI. The immunosensor revealed a wide range of linearity with a low detection limit of 0.02 ng mL^{-1}. Therefore, a competitive immunoassay was established between 17β-estradiol and the HRP–GO–Ab conjugates which showed a wide linear response to estradiol in the range 0.04–7.00 ng/mL and a limit of detection of 0.02 ng/mL (S/N = 3). The developed immunosensor was successfully applied for the detection of estradiol in real samples.

The detection of benzo[a] pyrene (BaP) was performed using a multi-enzyme antibody of RP-HCS secondary antibody immobilized on Fe_3O_4/PANI/Nafion sensor (Lin et al. 2012). The nanocomposite provided an active electron transfer pathway for reducing H_2O_2. The stable film of Fe_3O_4/PANI/Nafion not only immobilized biomolecules but also catalyzed the reduction of hydrogen peroxide which confirmed an accelerated electron transfer pathway of the platform. On the

basis of a competitive immunoassay, the current charge was found to be proportional to the logarithm of BaP concentration encompassing the range of 8 pM and 2 nM with the detection limit of 4 pM. Thus, the proposed immunosensor exhibited acceptable reproducibility and stability.

A label-free immunosensor has been designed for detecting low density lipoproteins (LDL) (Lin et al. 2012). The AuNPs−AgCl@PANI hybrid material was synthesized by reacting silver chloride@polyaniline (PANI) core−shell nanocomposites (AgCl@PANI) combined with Au nanoparticles (AuNPs). Apolipoprotein B-100 antibody was immobilized on the surface of Au–AgCl/PANI nanocomposite and the sensor performance was monitored via electrochemical impedance spectroscopy (EIS). The nanocomposite material provided a cover for high antibody loading due to the high surface-to-volume ratio. The poor conductivity of LDL and the negative charges performed brought about a shift in electron transfer resistance which facilitated its detection. The immunosensor had a very low detection limit (0.34 pg mL^{-1}) at an optimized condition, i.e., incubation time and incubation temperature (50 min, 37 °C). PANI based hybrid materials provide a useful transducer to which the immunochemical reactions can be coupled. The advantages of fabricated immunosensor include simplicity of design and tunability of PANI properties by a combination of nanomaterials, thus, making facile label-free detection of antigens possible.

6.3.5.4 DNA Based Biosensors

PANI based biosensors were also employed for the detection of DNA to provide high sensitivity as well as accurate and rapid detection. These biosensors have been used in the fields of forensics, biological warfare detection, gene analysis, and DNA diagnostics (Dhand et al. 2011). A single stranded DNA (ssDNA) probe immobilized on the surface of transducer recognizes its complementary DNA target by hybridization. A PANI-graphite oxide based nanocomposite was fabricated on a carbon paste electrode (CPE) for monitoring DNA hybridization (Wu et al. 2005). Both ssDNA and dsDNA (double-strand DNA) change the redox properties of the nanocomposite electrode. To monitor hybridization and detect the complementary ssDNA of the biosensor, Square wave voltammetry (SWV) was utilized. The responses were influenced by pH and incubation time. DNA sensing behaviour of graphene and PANI nanocomposites have also been reported by other researchers (Bo et al. 2011; Du et al. 2012). Graphene sheets on GCE followed by electropolymerization of PANI and electrodeposition of Au nanoparticles were employed as a layered biosensor in order to detect BCR/ABL fusion gene in chronic myelogenous leukemia (CML) (Wang et al. 2014). After hybridization, the 30 -biotin site face moved away from the electrode surface, binding the streptavidin–alkaline phosphatase. The hydrolysis of 1-naphthyl phosphate to 1-naphthol was monitored using DPV. The biosensor showed high selectivity having a detection limit of 2.11 pM.

Another label-free electrochemical DNA sensor using PPY/PANI/ Au nanocomposite was employed as ssDNA labeled with 6-mercapto-1- hexane for hybridization (Wilson et al. 2012). Compared to the lone Au nanoparticle based transducer, the biopolymer improved the hybridization efficiency of the ssDNA, highly sensitive towards the complementary ssDNA with a low detection limit of 1013 M. Forster and co-workers used A PANI nanocomposite with surface deposited Au nanoparticles as DNA biosensor (Spain et al. 2011, 2013). In one of their reports, thiolated ssDNA, which act as complementary to a sequence of Staphylococcus aureus, was immobilized onto the surface of the nanocomposite. HRP labeled probe strand was hybridized to an unbound section of the capture strand. The target concentration was determined by measuring current during reduction of benzoquinone through HRP.

PANI/MWCNT nanocomposite was prepared for detecting the phosphinothricin acetyltransferase gene (PAT), one of the screening detection genes for the transgenic plants (Yang et al. 2009; Prathap et al. 2013). A ssDNA probe was immobilized onto the nanocomposite and hybridization was detected via EIS. It was successfully applied to the real sample of genetically modified soybean.

PANI/ZrO_2 nanocomposites were used for detecting polytyrosine Phosphinothricin acetyl transferase (PAT) (Yang et al. 2012). The nanocomposite aided in ssDNA immobilization and hybridization was investigated by CV and EIS techniques. The electron transfer resistance was found to increase with the increase in the concentration of target DNA. It was also found that nanocomposites, i.e., PANI- MWCNT and PANI-ZrO_2, exhibited the same detection limit.

In another study, the detection of a DNA base (i.e., guanine, adenine, thymine, and cytosine) was performed using PANI/MnO_2 nanocomposite (Prathap et al. 2013). Radhakrishnan et al., reported the fabrication of PPY/PANI nanocomposite with ssDNA immobilized onto it via glutaraldehyde, using methyl blue dye as an electrochemical indicator (Radhakrishnan et al. 2013). The biosensor showed remarkable sensitivity with a detection limit of 50 fM. PANI based DNA biosensors were also utilized for detection of pesticide.

A nucleic acid based biosensor was reported by Prabhakar et al., for pesticide detection (Prabhakar et al. 2008). The calf thymus dsDNA immobilized onto PANI-polyvinyl sulphonate (PVS) nanocomposite showed superior stability. Hybridization with the target DNA changes the doping level of PANI, and as a result alters its conductivity. PANI based nanocomposites and their sensing applications presented in Table 6.2.

6.4 Conclusion

PANI based nanocomposite ion-exchange materials and nanocomposites have demonstrated excellent behaviour towards detection and sensing of gases. Also, these nano-materials have facilitated the immobilization of range of bioreceptors (such as enzymes, antigen–antibodies, and nucleic acids) onto their surfaces for exposure of

Table 6.2 PANI based nanocomposite ion-exchange materials and their sensing applications

S. no	Nanocomposite	Analysis	Application	Reference
1.	PANI-Pd	UV-vis., TEM	Methanol	Athawale et al. (2006)
2.	PANI-Ag	UV-vis., TEM	Ethanol	Choudhury (2009)
3.	PANI-Ag	SEM, TEM	Triethylamine, toluene	Li et al. (2013a)
4.	PANI-Cu	TEM, FTIR	Chloroform	Sharma et al. (2002)
5.	PANI-TiO_2	XRD, SEM	NH_3	Pawar et al. (2011)
6.	PANI-SnO_2	FTIR, XRD, SEM, AFM	NH_3	Deshpande et al. (2009)
7.	PANI-PMMA	SEM, RAMAN	NH_3	Zhang et al. (2014)
8.	PANI-NiTSPc	SEM, AFM, RAMAN, FTIR	NH_3	Zhihua et al. (2016)
9.	PANI-$CuCl_2$	UV-vis., SERS	H_2S	Crowley et al. (2010)
10.	PANI–CdS	XRD, SEM	H_2S	Raut et al. (2012)
11.	PANI–Au	SEM	H_2S	Shirsat et al. (2009)
12.	n-CdSe-p-PANI	SEM, AFM	LPG	Joshi et al. (2007)
13.	PANI/g-Fe_2O_3	FTIR, UV-vis. XRD, FESEM	LPG	Sen et al. (2014)
14.	PANI-TiO2	XRD, SEM	LPG	Dhawale et al. (2008)
15.	PANI-CdSe	XRD, SEM	LPG	Dhawale et al. (2010a)
16.	PANI-ZnO	XRD, SEM, TGA	LPG	Dhawale et al. (2010b)
17.	PANI-ZnO	by XRD, SEM, TGA and UV-Vis	Humidity	Shukla et al. (2012)
18.	PANI-Co	XRD, SEM, FTIR	Humidity	Vijayan et al. (2008)
19.	PANI-Ag	XRD, UV-vis. FTIR, SEM	Humidity	Vijayan et al. (2008)
20.	PANI–β-$AgVO_3$	FESEM, HRTEM, AFM analyses. FTIR and EDAX	Humidity	Diggikar et al. (2013)
21.	PANI-In_2O_3	FTIR, SEM	CH_4, CO	Yan et al. (2009)
22.	PANI-SnO_2	UV-vis., SEM	CO	Ram et al. (2005b)
23.	PANI-SWCNT	FTIR, SEM	CO	Kim et al. (2010)

(continued)

Table 6.2 (continued)

S. no	Nanocomposite	Analysis	Application	Reference
24.	PANI-TiO_2-MWCNT	XRD, FESEM	NO	Yun et al. (2013)
25.	PANI- SnO_2–ZnO	FTIR, XRD, FESEM	NO_2	Xu et al. (2013b)
26.	MWNT-PANI and TiO_2-PANI	XRD, SEM	H_2	Srivastava et al. (2010)
27.	PANI-WO_3	SEM, TEM, XRD	H_2	Sadek et al. (2008)
28.	PANI-PtO_2	–	H_2	Conn et al. (1998)
29.	PANI-ClAlPc	–	CO	Azim-Araghi and Jafari (2010)
30.	PANI-Au	TEM	Glucose	Xian et al. (2006)
31.	Graphene/PANI/Au	FTIR, SEM	Glucose	Fu and Yu (2014)
32.	PANI–TiO_2	FTIR, XRD, TEM	Glucose	Zhu et al. (2015)
33.	PANI (PAA)-Au	–	Salbutamol	Huang et al. (2011)
34.	GO-PANI-CdSe	TEM	Interleukin-6	Liu et al. (2013)
35.	PANI/Au	UV-vis., SEM, TEM, AFM	Prostate-specific antigen	Dey et al. (2012)
36.	Au-PANI-cMWCNTs-chitosan	XRD, SEM	Chlorpyrifos	Sun et al. (2013)
37.	GR–PANI	SEM, FTIR, UV-vis.	Estradiol	Li et al. (2013b)
38.	Fe_3O_4-PANI-Nafion	UV-vis., TEM	Benzo[a] pyrene	Lin et al. (2012)
39.	AuNPs−AgCl@PANI	TEM, XRD, TGA, XPS	Lipoproteins	Lin et al. (2012)
40.	PANI-GO	–	DNA hybridization	Wu et al. (2005)
41.	Au-PANI on GCE	SEM	BCR/ABL fusion gene (in chronic myelogenous leukemia)	Wang et al. (2014)
42.	PPY-PANI-Au	SEM	DNA hybridization	Wilson et al. (2012)
43.	PANI-MWCNT	SEM	Phosphinothricin acetyltransferase gene	Yang et al. (2009)
44.	PANI-cMWCNTs	XRD, SEM, TEM, FTIR	DNA bases	(Prathap et al. 2013)

an array of biological agents via a combination of biochemical and electrochemical reactions. However, their commercialization remains a severe obstacle to scientific community because PANI itself suffers from some drawbacks, including their synthesis. Controlled synthesis of PANI at optimized pH and temperature is necessary to avoid secondary growth while retaining its nanostructure. In addition, dopant and its electronic properties play a crucial role in the synthesis of PANI. PANI can be highly conducting, self-doped, and/or soluble in aqueous and non-aqueous organic solvents based on dopant nature. PANI in doped form can have a relatively short shelf life. Besides, merging the secondary component in PANI showed a synergistic effect in improving its shelf life in doped form, and various other properties, and further applications. Therefore, fabrication of PANI nanocomposites with extended experience in doped structure is essential as far as its durability is concerned. Compared to pure PANI, its nanocomposites have shown improved characteristics regarding thermal and chemical stability. Moreover, PANI based nanocomposites have been used for safer, selective and sensitive detection of number combustible and toxic gases at room temperature. These materials halt the response variation resulting from structural changes in the sensing material at elevated temperatures as well as prevent sensor instability.

One of the disadvantages of a large number of nanocomposites based sensors is that their response is influenced by humidity which may result in false responses in the material. Thus, development of PANI supported nanocomposites resistant to humidity is one of the critical challenges. The enhancement in electron transfer capability of PANI nanocomposites is found attractive for detecting biological agents. Immobilization of biological agents onto PANI transducers becomes possible after incorporation of a secondary component with PANI. A better interaction between the components of the nanocomposite will improve the effectiveness and performance of the sensor. In this respect, there is a definite need for new approaches in order to understand the mechanism involved in analyte sensing by PANI and its various exciting nanocomposites for fabricating and commercializing highly selective sensors for specific agents.

Acknowledgement The authors would like to express their appreciations to Science and Engineering Research Board (DST) fast tract young scientist scheme (SB/FT/CS-122/2014) for providing Postdoctoral Fellowship to Mohammad Shahadat.

References

Abdulla S, Mathew TL, Pullithadathil B (2015) Highly sensitive, room temperature gas sensor based on polyaniline-multiwalled carbon nanotubes (PANI/MWCNTs) nanocomposite for trace-level ammonia detection. Sensors Actuators B Chem 221:1523–1534

Adams P et al (1996) Low temperature synthesis of high molecular weight polyaniline. Polymer 37 (15):3411–3417

Ampuero S, Bosset J (2003) The electronic nose applied to dairy products: a review. Sensors Actuators B Chem 94(1):1–12

Ansari MO, Mohammad F (2011) Thermal stability, electrical conductivity and ammonia sensing studies on p-toluenesulfonic acid doped polyaniline: titanium dioxide (pTSA/Pani: TiO2) nanocomposites. Sensors Actuators B Chem 157(1):122–129

Ansari MO et al (2013) Thermal stability in terms of DC electrical conductivity retention and the efficacy of mixing technique in the preparation of nanocomposites of graphene/polyaniline over the carbon nanotubes/polyaniline. Compos Part B 47:155–161

Ansari MO et al (2014) Ammonia vapor sensing and electrical properties of fibrous multi-walled carbon nanotube/polyaniline nanocomposites prepared in presence of cetyltrimethylammonium bromide. J Ind Eng Chem 20(4):2010–2017

Arrad O, Sasson Y (1989) Commercial ion exchange resins as catalysts in solid-solid-liquid reactions. J Org Chem 54(21):4993–4998

Arsat R et al (2011) Hydrogen gas sensor based on highly ordered polyaniline/multiwall carbon nanotubes composite. Sens Lett 9(2):940–943

Athawale AA, Kulkarni MV (2000) Polyaniline and its substituted derivatives as sensor for aliphatic alcohols. Sensors Actuators B Chem 67(1):173–177

Athawale AA, Bhagwat S, Katre PP (2006) Nanocomposite of Pd–polyaniline as a selective methanol sensor. Sensors Actuators B Chem 114(1):263–267

Ayad MM, El-Hefnawey G, Torad NL (2009) A sensor of alcohol vapours based on thin polyaniline base film and quartz crystal microbalance. J Hazard Mater 168(1):85–88

Azim-Araghi M, Jafari M (2010) Electrical and gas sensing properties of polyaniline-chloroaluminium phthalocyanine composite thin films. Eur Phys J Appl Phys 52(01):10402

Baraton M-I (2008) Sensors for environment, health and security: advanced materials and technologies. Springer, Dordrecht

Bo Y et al (2011) A novel electrochemical DNA biosensor based on graphene and polyaniline nanowires. Electrochim Acta 56(6):2676–2681

Bushra R et al (2014) Synthesis, characterization, antimicrobial activity and applications of polyanilineTi (IV) arsenophosphate adsorbent for the analysis of organic and inorganic pollutants. J Hazard Mater 264:481–489

Castro M et al (2009) Carbon nanotubes/poly (ε-caprolactone) composite vapour sensors. Carbon 47(8):1930–1942

Cavallo P et al (2015) Understanding the sensing mechanism of polyaniline resistive sensors. Effect of humidity on sensing of organic volatiles. Sensors Actuators B Chem 210:574–580

Chaudhary V, Kaur A (2015) Enhanced room temperature sulfur dioxide sensing behaviour of in situ polymerized polyaniline–tungsten oxide nanocomposite possessing honeycomb morphology. RSC Adv 5(90):73535–73544

Choudhury A (2009) Polyaniline/silver nanocomposites: dielectric properties and ethanol vapour sensitivity. Sensors Actuators B Chem 138(1):318–325

Clark LC, Lyons C (1962) Electrode systems for continuous monitoring in cardiovascular surgery. Ann N Y Acad Sci 102(1):29–45

Conn C et al (1998) A polyaniline-based selective hydrogen sensor. Electroanalysis 10(16):1137–1141

Crowley K et al (2010) Fabrication of polyaniline-based gas sensors using piezoelectric inkjet and screen printing for the detection of hydrogen sulfide. Sens J IEEE 10(9):1419–1426

Deshpande N et al (2009) Studies on tin oxide-intercalated polyaniline nanocomposite for ammonia gas sensing applications. Sensors Actuators B Chem 138(1):76–84

Dey A et al (2012) Mediator free highly sensitive polyaniline–gold hybrid nanocomposite based immunosensor for prostate-specific antigen (PSA) detection. J Mater Chem 22(29):14763–14772

Dhand C et al (2011) Recent advances in polyaniline based biosensors. Biosens Bioelectron 26 (6):2811–2821

Dhawale D et al (2008) Room temperature liquefied petroleum gas (LPG) sensor based on p-polyaniline/n-TiO2 heterojunction. Sensors Actuators B Chem 134(2):988–992

Dhawale D et al (2010a) Room temperature LPG sensor based on n-CdS/p-polyaniline heterojunction. Sensors Actuators B Chem 145(1):205–210
Dhawale D et al (2010b) Room temperature liquefied petroleum gas (LPG) sensor. Sensors Actuators B Chem 147(2):488–494
Dhingra M et al (2013) Impact of interfacial interactions on optical and ammonia sensing in zinc oxide/polyaniline structures. Bull Mater Sci 36(4):647–652
Di W, Ivaska A (2006) Electrochemical biosensors based on polyaniline. Chem Anal 51(6):839–852
Diggikar RS et al (2013) Formation of multifunctional nanocomposites with ultrathin layers of polyaniline (PANI) on silver vanadium oxide (SVO) nanospheres by in situ polymerization. J Mater Chem A 1(12):3992–4001
Dimitriev O (2003) Interaction of polyaniline and transition metal salts: formation of macromolecular complexes. Polym Bull 50(1–2):83–90
Docquier N, Candel S (2002) Combustion control and sensors: a review. Prog Energy Combust Sci 28(2):107–150
Du M et al (2012) Fabrication of DNA/graphene/polyaniline nanocomplex for label-free voltammetric detection of DNA hybridization. Talanta 88:439–444
Dubbe A (2003) Fundamentals of solid state ionic micro gas sensors. Sensors Actuators B Chem 88 (2):138–148
Feng J, MacDiarmid A (1999) Sensors using octaaniline for volatile organic compounds. Synth Met 102(1):1304–1305
Fu L, Yu A (2014) Carbon nanotubes based thin films: fabrication, characterization and applications. Rev Adv Mater Sci 36:40–61
Fuke MV et al (2008) Evaluation of co-polyaniline nanocomposite thin films as humidity sensor. Talanta 76(5):1035–1040
Fuke MV et al (2009) Ag-polyaniline nanocomposite cladded planar optical waveguide based humidity sensor. J Mater Sci Mater Electron 20(8):695–703
Gangopadhyay R, De A (2000) Conducting polymer nanocomposites: a brief overview. Chem Mater 12(3):608–622
Genies E et al (1990) Polyaniline: a historical survey. Synth Met 36(2):139–182
Gopalan AI et al (2009) An electrochemical glucose biosensor exploiting a polyaniline grafted multiwalled carbon nanotube/perfluorosulfonate ionomer–silica nanocomposite. Biomaterials 30(30):5999–6005
Hasan M et al (2015) Ammonia sensing and DC electrical conductivity studies of p-toluene sulfonic acid doped cetyltrimethylammonium bromide assisted V2O5@ polyaniline composite nanofibers. J Ind Eng Chem 22:147–152
Hoa D et al (1992) A biosensor based on conducting polymers. Anal Chem 64(21):2645–2646
Hsu YF et al (2008) Undoped p-type ZnO Nanorods synthesized by a hydrothermal method. Adv Funct Mater 18(7):1020–1030
Hu H et al (2002) Adsorption kinetics of optochemical NH 3 gas sensing with semiconductor polyaniline films. Sensors Actuators B Chem 82(1):14–23
Huang W-S, Humphrey BD, MacDiarmid AG (1986) Polyaniline, a novel conducting polymer. Morphology and chemistry of its oxidation and reduction in aqueous electrolytes. J Chem Soc Faraday Trans 82(8):2385–2400
Huang J et al (2011) Electrochemical immunosensor based on polyaniline/poly (acrylic acid) and Au-hybrid graphene nanocomposite for sensitivity enhanced detection of salbutamol. Food Res Int 44(1):92–97
Imisides M, John R, Wallace G (1996) Microsensors based on conducting polymers. ChemTech 26 (5):19–25
Jain S et al (2003) Humidity sensing with weak acid-doped polyaniline and its composites. Sensors Actuators B Chem 96(1):124–129
Joshi S, Lokhande C, Han S-H (2007) A room temperature liquefied petroleum gas sensor based on all-electrodeposited n-CdSe/p-polyaniline junction. Sensors Actuators B Chem 123(1):240–245

Kaur B, Srivastava R (2015) Simultaneous determination of epinephrine, paracetamol, and folic acid using transition metal ion-exchanged polyaniline–zeolite organic–inorganic hybrid materials. Sensors Actuators B Chem 211:476–488

Khan AA (2006) Applications of Hg (II) sensitive polyaniline Sn (IV) phosphate composite cation-exchange material in determination of Hg^{2+} from aqueous solutions and in making ion-selective membrane electrode. Sensors Actuators B Chem 120(1):10–18

Khan AA, Baig U (2013a) Electrical conductivity and ammonia sensing studies on in situ polymerized poly (3-methythiophene)–titanium (IV) molybdophosphate cation exchange nanocomposite. Sensors Actuators B Chem 177:1089–1097

Khan AA, Baig U (2013b) Electrical conductivity and humidity sensing studies on synthetic organic–inorganic poly-o-toluidine–titanium (IV) phosphate cation exchange nanocomposite. Solid State Sci 15:47–52

Khan AA, Khalid M, Niwas R (2010a) Humidity and ammonia vapor sensing applications of polyaniline–polyacrylonitrile composite films. Sci Adv Mater 2(4):474–480

Khan AA, Khalid M, Baig U (2010b) Synthesis and characterization of polyaniline–titanium (IV) phosphate cation exchange composite: methanol sensor and isothermal stability in terms of DC electrical conductivity. React Funct Polym 70(10):849–855

Khan AA, Baig U, Khalid M (2011) Ammonia vapor sensing properties of polyaniline–titanium (IV) phosphate cation exchange nanocomposite. J Hazard Mater 186(2):2037–2042

Khan AA, Baig U, Khalid M (2013a) Electrically conductive polyaniline-titanium (IV) molybdophosphate cation exchange nanocomposite: synthesis, characterization and alcohol vapour sensing properties. J Ind Eng Chem 19(4):1226–1233

Khan AA et al (2013b) Ion-exchange and humidity sensing properties of poly-o-anisidine sn (IV) arsenophosphate nano-composite cation-exchanger. J Environ Chem Eng 1(3):310–319

Khuspe G et al (2013) Ammonia gas sensing properties of CSA doped PANi-SnO2 nanohybrid thin films. Synth Met 185:1–8

Kim I et al (2010) Gas sensor for CO and NH 3 using polyaniline/CNTs composite at room temperature. In: Nanotechnology (IEEE-NANO), 10th IEEE conference on 2010, IEEE

Koul S, Chandra R (2005) Mixed dopant conducting polyaniline reusable blend for the detection of aqueous ammonia. Sensors Actuators B Chem 104(1):57–67

Le TH et al (2013) Electrosynthesis of polyaniline–mutilwalled carbon nanotube nanocomposite films in the presence of sodium dodecyl sulfate for glucose biosensing. Adv Nat Sci Nanosci Nanotechnol 4(2):025014

Li Z-F et al (2013a) Understanding the response of nanostructured polyaniline gas sensors. Sensors Actuators B Chem 183:419–427

Li J et al (2013b) Electrochemical immunosensor based on graphene–polyaniline composites and carboxylated graphene oxide for estradiol detection. Sensors Actuators B Chem 188:99–105

Lin M et al (2012) Electrochemical immunoassay of benzo [a] pyrene based on dual amplification strategy of electron-accelerated Fe3O4/polyaniline platform and multi-enzyme-functionalized carbon sphere label. Anal Chim Acta 722:100–106

Liu P-Z et al (2013) Electrochemiluminescence immunosensor based on graphene oxide nanosheets/polyaniline nanowires/CdSe quantum dots nanocomposites for ultrasensitive determination of human interleukin-6. Electrochim Acta 113:176–180

Lowe CR (1984) Biosensors. Trends Biotechnol 2(3):59–65

Malinauskas A et al (2004) Electrochemical response of ascorbic acid at conducting and electrogenerated polymer modified electrodes for electroanalytical applications: a review. Talanta 64(1):121–129

Matsuguchi M et al (2002) Effect of NH 3 gas on the electrical conductivity of polyaniline blend films. Synth Met 128(1):15–19

Muhammad-Tahir Z, Alocilja EC (2003) A conductometric biosensor for biosecurity. Biosens Bioelectron 18(5):813–819

Nabi S et al (2010) Development of composite ion-exchange adsorbent for pollutants removal from environmental wastes. Chem Eng J 165(2):405–412

Nabi S et al (2011a) Synthesis and characterization of nano-composite ion-exchanger; its adsorption behavior. Colloids Surf B: Biointerfaces 87(1):122–128
Nabi S et al (2011b) Heavy-metals separation from industrial effluent, natural water as well as from synthetic mixture using synthesized novel composite adsorbent. Chem Eng J 175:8–16
Nabi S et al (2011c) Synthesis and characterization of polyanilineZr (IV) sulphosalicylate composite and its applications (1) electrical conductivity, and (2) antimicrobial activity studies. Chem Eng J 173(3):706–714
Navale S et al (2014) Camphor sulfonic acid doped PPy/α-Fe2O3 hybrid nanocomposites as NO2 sensors. RSC Adv 4(53):27998–28004
Novák P et al (1997) Electrochemically active polymers for rechargeable batteries. Chem Rev 97 (1):207–282
Ozdemir C et al (2010) Electrochemical glucose biosensing by pyranose oxidase immobilized in gold nanoparticle-polyaniline/AgCl/gelatin nanocomposite matrix. Food Chem 119(1):380–385
Parvatikar N et al (2006) Electrical and humidity sensing properties of polyaniline/WO3 composites. Sensors Actuators B Chem 114(2):599–603
Patil S et al (2011) Fabrication of polyaniline-ZnO nanocomposite gas sensor. Sens Transducer 134 (11):120
Pawar S et al (2011) Fabrication of polyaniline/TiO2 nanocomposite ammonia vapor sensor. J Nano Electron Phys 3(1):1056
Prabhakar N et al (2008) Improved electrochemical nucleic acid biosensor based on polyaniline-polyvinyl sulphonate. Electrochim Acta 53(12):4344–4350
Prathap MA, Srivastava R, Satpati B (2013) Simultaneous detection of guanine, adenine, thymine, and cytosine at polyaniline/MnO2 modified electrode. Electrochim Acta 114:285–295
Radhakrishnan S et al (2013) Polypyrrole nanotubes–polyaniline composite for DNA detection using methylene blue as intercalator. Anal Methods 5(4):1010–1015
Raj AD et al (2010) Self assembled V2O5 nanorods for gas sensors. Curr Appl Phys 10(2):531–537
Ram MK, Yavuz O, Aldissi M (2005a) NO2 gas sensing based on ordered ultrathin films of conducting polymer and its nanocomposite. Synth Met 151(1):77–84
Ram MK et al (2005b) CO gas sensing from ultrathin nano-composite conducting polymer film. Sensors Actuators B Chem 106(2):750–757
Raman NK, Anderson MT, Brinker CJ (1996) Template-based approaches to the preparation of amorphous, nanoporous silicas. Chem Mater 8(8):1682–1701
Raut B et al (2012) Novel method for fabrication of polyaniline–CdS sensor for H2S gas detection. Measurement 45(1):94–100
Riegel J, Neumann H, Wiedenmann H-M (2002) Exhaust gas sensors for automotive emission control. Solid State Ionics 152:783–800
Rujisamphan N et al (2016) Co-sputtered metal and polymer nanocomposite films and their electrical responses for gas sensing application. Appl Surf Sci 368:114–121
Sadek A et al (2006) A layered surface acoustic wave gas sensor based on a polyaniline/In2O3 nanofibre composite. Nanotechnology 17(17):4488
Sadek A et al (2008) A polyaniline/WO3 nanofiber composite-based ZnO/64 YX LiNbO3 SAW hydrogen gas sensor. Synth Met 158(1):29–32
Sajjan K et al (2013) Humidity sensing property of polyaniline-cromium oxide nanocomposites. In: Proceeding of international conference on recent trends in applied physics and material science: RAM 2013, AIP Publishing
Santhanam K, Gupta N (1993) Conducting-polymer electrodes in batteries. TRIP 1:284–289
Sarfraz J et al (2013) Printed hydrogen sulfide gas sensor on paper substrate based on polyaniline composite. Thin Solid Films 534:621–628
Sen T et al (2014) Polyaniline/γ-Fe2O3 nanocomposite for room temperature LPG sensing. Sensors Actuators B Chem 190:120–126
Shahadat M et al (2012) Synthesis, characterization, photolytic degradation, electrical conductivity and applications of a nanocomposite adsorbent for the treatment of pollutants. RSC Adv 2 (18):7207–7220

Shahadat M et al (2015) Titanium-based nanocomposite materials: a review of recent advances and perspectives. Colloids Surf B: Biointerfaces 126:121–137
Shahadat M et al (2017) A critical review on the prospect of polyaniline-grafted biodegradable nanocomposite. Adv Colloid Interf Sci 249:2–16
Sharma S et al (2002) Chloroform vapour sensor based on copper/polyaniline nanocomposite. Sensors Actuators B Chem 85(1):131–136
Shirsat MD et al (2009) Polyaniline nanowires-gold nanoparticles hybrid network based chemiresistive hydrogen sulfide sensor. Appl Phys Lett 94(8):083502
Shukla S et al (2012) Fabrication of electro-chemical humidity sensor based on zinc oxide/polyaniline nanocomposites. Adv Mater Lett 3(5):421–425
Singh V et al (2008) Synthesis and characterization of polyaniline–carboxylated PVC composites: application in development of ammonia sensor. Sensors Actuators B Chem 132(1):99–106
Singla M, Awasthi S, Srivastava A (2007) Humidity sensing; using polyaniline/Mn3O4 composite doped with organic/inorganic acids. Sensors Actuators B Chem 127(2):580–585
Spain E et al (2011) High sensitivity DNA detection using gold nanoparticle functionalised polyaniline nanofibres. Biosens Bioelectron 26(5):2613–2618
Spain E, Keyes TE, Forster RJ (2013) Vapour phase polymerised polyaniline–gold nanoparticle composites for DNA detection. J Electroanal Chem 711:38–44
Srivastava S et al (2010) TiO_2/PANI And MWNT/PANI composites thin films For hydrogen gas sensing. In: AIP conference proceedings
Sun X, Qiao L, Wang X (2013) A novel immunosensor based on Au nanoparticles and polyaniline/multiwall carbon nanotubes/chitosan nanocomposite film functionalized interface. Nano-Micro Lett 5(3):191–201
Sutar D et al (2007) Preparation of nanofibrous polyaniline films and their application as ammonia gas sensor. Sensors Actuators B Chem 128(1):286–292
Syed AA, Dinesan MK (1991) Review: polyaniline – a novel polymeric material. Talanta 38 (8):815–837
Tai H et al (2007) Fabrication and gas sensitivity of polyaniline–titanium dioxide nanocomposite thin film. Sensors Actuators B Chem 125(2):644–650
Tovide O et al (2014) Graphenated polyaniline-doped tungsten oxide nanocomposite sensor for real time determination of phenanthrene. Electrochim Acta 128:138–148
Vatutsina O et al (2007) A new hybrid (polymer/inorganic) fibrous sorbent for arsenic removal from drinking water. React Funct Polym 67(3):184–201
Verma SK et al (2015) Poly (m-aminophenol)/functionalized multi-walled carbon nanotube nanocomposite based alcohol sensors. Sensors Actuators B Chem 219:199–208
Vijayan A et al (2008) Optical fibre based humidity sensor using co-polyaniline clad. Sensors Actuators B Chem 129(1):106–112
Wang X et al (2012) Synthesis of nestlike ZnO hierarchically porous structures and analysis of their gas sensing properties. ACS Appl Mater Interfaces 4(2):817–825
Wang L et al (2014) Graphene sheets, polyaniline and AuNPs based DNA sensor for electrochemical determination of BCR/ABL fusion gene with functional hairpin probe. Biosens Bioelectron 51:201–207
Wilson J et al (2012) Polypyrrole–polyaniline–Au (PPy–PANi–Au) nano composite films for label-free electrochemical DNA sensing. Sensors Actuators B Chem 171:216–222
Wu J et al (2005) A biosensor monitoring DNA hybridization based on polyaniline intercalated graphite oxide nanocomposite. Sensors Actuators B Chem 104(1):43–49
Xian Y et al (2006) Glucose biosensor based on Au nanoparticles–conductive polyaniline nanocomposite. Biosens Bioelectron 21(10):1996–2000
Xu D-M et al (2013a) Multilayer films of layered double hydroxide/polyaniline and their ammonia sensing behavior. J Hazard Mater 262:64–70
Xu H et al (2013b) NO 2 gas sensing with SnO 2–ZnO/PANI composite thick film fabricated from porous nanosolid. Sensors Actuators B Chem 176:166–173

Yan X et al (2009) Preparation and characterization of polyaniline/indium (III) oxide (PANi/In2O3) nanocomposite thin film. In: 4th international symposium on advanced optical manufacturing and testing technologies: advanced optical manufacturing technologies. International Society for Optics and Photonics

Yang T et al (2009) Synergistically improved sensitivity for the detection of specific DNA sequences using polyaniline nanofibers and multi-walled carbon nanotubes composites. Biosens Bioelectron 24(7):2165–2170

Yang J, Wang X, Shi H (2012) An electrochemical DNA biosensor for highly sensitive detection of phosphinothricin acetyltransferase gene sequence based on polyaniline-(mesoporous nanozirconia)/poly-tyrosine film. Sensors Actuators B Chem 162(1):178–183

Yun J, Jeon S, Kim H-I (2013) Improvement of NO gas sensing properties of polyaniline/MWCNT composite by photocatalytic effect of TiO2. J Nanomater 2013:3

Zhang H-D et al (2014) High-sensitivity gas sensors based on arranged polyaniline/PMMA composite fibers. Sensors Actuators A Phys 219:123–127

Zhihua L et al (2016) Fast response ammonia sensor based on porous thin film of polyaniline/sulfonated nickel phthalocyanine composites. Sensors Actuators B Chem 226:553–562

Zhong H et al (2011) In situ chemo-synthesized multi-wall carbon nanotube-conductive polyaniline nanocomposites: characterization and application for a glucose amperometric biosensor. Talanta 85(1):104–111

Zhu J et al (2015) Preparation of polyaniline–TiO2 nanotube composite for the development of electrochemical biosensors. Sensors Actuators B Chem 221:450–457